

On the importance of the heat release rate in numerical simulations of fires in mechanically ventilated air-tight enclosures

Bart Merci*, Junyi Li, Georgios Maragkos

Ghent University, Department of Structural Engineering and Building Materials, Ghent, Belgium

Abstract

A fire in a compartment with limited ventilation can cause a significant pressure rise, up to hundreds of Pascal. This is important in practice, as the pressure rise can cause damage or hinder evacuation, but also from the perspective of fire safety science. From the energy balance, taking into account the interaction between compartment pressure, fire dynamics and mechanical ventilation, the importance of the net heat gained per unit time in the gas phase is well recognized. This leads to the need to accurately quantify the heat release rate inside the compartment as a function of time. It is explained that scaling of the transient phenomena is not straightforward. The paper then focuses on numerical simulations, in particular on CFD in the gas phase. An overview is presented of different existing approaches for turbulent combustion modelling in turbulent buoyancy-driven flames with low values of scalar dissipation rate, typical for fire flames. A dynamic approach for modelling turbulent combustion, and the coupling with radiation modelling, is briefly discussed. Extinction and re-ignition are discussed extensively, in the context of reduced ventilation conditions. Finally, low-frequency oscillatory behavior in mechanically ventilated air-tight compartments is addressed. It is argued that CFD simulations are a very valuable tool to gain further insight in this phenomenon. Suggestions for future research are formulated.

Keywords: compartment fire; mechanical ventilation; energy balance; pressure; fire dynamics; CFD

*Corresponding author.

1. Introduction

In air-tight compartments, as encountered in passive houses or some industrial facilities, there is a potential risk of substantial fire-induced pressure variation. Such pressure variations have been long ignored in the context of compartment fire dynamics research, because they are negligible as long as there is a significant amount of ventilation openings or leakage, which is often the case. However, the increasing popularity of passive houses (leading to reduced energy consumption) and the importance of safety in, e.g., nuclear facilities, has induced growing attention for fire-induced pressure variations, in particular in combination with mechanical ventilation. In residential context, strong pressure variation can hinder evacuation (if doors can no longer be opened) or cause damage (e.g., window breakage or potentially even more serious structural damage), while in an industrial environment often mechanical damage or a loss of confinement can be primary concerns. This illustrates the practical relevance of the topic of this paper.

In [1, 2], it is illustrated that heptane pool and polyurethane foam fires in relatively closed compartments can induce significant over- and under-pressures. These observations align well with the experimental data as reported in, e.g., [3, 4]. Strong pressure variations and the consequence on the opening of doors have also been reported in [5, 6], using zone model calculations. Experimental data, using wood cribs, are provided in [7-9].

Although overall air-tight compartments have not received much attention yet, this is a relevant canonical problem from a fire safety science point of view as well. The pressure rise is too limited to have a significant direct impact on the combustion and heat transfer processes, but accurate prediction of the transient (and possibly oscillatory) pressure evolution requires precise knowledge of the evolutions of heat release rate (HRR) and heat losses per unit time. Particularly the HRR is strongly affected by turbulent combustion, which depends on the ventilation conditions and the fuel supply rate (which may depend on evaporation or pyrolysis processes, and hence on heat feedback from the flames). All these processes, and their coupling, make this an interesting problem from a fire safety science point of view.

A fundamental understanding of the different physics involved in scenarios with mechanically ventilated air-tight enclosures is indeed crucial, and many modelling challenges need to be addressed in the quest of developing accurate models that could be used for predictive fire modelling. More specifically, there is an intricate coupling of the different physics involved in the gas phase, which cannot be easily decoupled, providing the necessary heat feedback to the fuel surface: accurate modelling of combustion (including flame extinction and re-ignition), combined with radiation and soot modelling, is important with respect to the predicted HRR. In general, a stepwise methodology is needed in order to develop a reliable and accurate CFD framework for numerical testing of such fire-

related scenarios. Decoupling and validating the gas and liquid/solid phases separately is of great importance to have confidence in the modelling approaches and to avoid compensating errors when complex scenarios are considered. The present paper focuses on the gas phase only.

The structure of this paper is as follows. The next section addresses the general discussion of the pressure evolution in case of fire in mechanically ventilated air-tight enclosures. It is highlighted that detailed reliable information on the evolution of the HRR is key. This holds for experiments as well as numerical simulations. Therefore, subsequently, model choices in CFD simulations are addressed in more detail, with specific focus on the HRR predictions. CFD simulations are argued to be useful in ongoing research in fire safety science. This is discussed in the final section of the paper, for the phenomenon of low-frequency oscillatory behavior, as observed in mechanically ventilated airtight compartment fires in certain circumstances. Finally, some conclusions and perspectives are formulated.

2. Pressure evolution: the importance of the heat release rate

2.1. General discussion

The fire-induced pressure variation can be derived from the energy conservation law, as explained in, e.g., [3, 10, 11]:

$$\frac{V}{\gamma - 1} \frac{d}{dt} p = \dot{Q}_f - \dot{Q}_w - \dot{Q}_v \quad (1)$$

where p is the spatial average compartment pressure (Pa); V is the compartment volume (m^3); γ is the gas isentropic coefficient; \dot{Q}_f , \dot{Q}_v and \dot{Q}_w represent the fire heat release rate (HRR) (W), the heat loss (which could be a net gain, though) through ventilation flows (W) and the wall (boundary) heat losses (W), respectively. These quantities are integrated over the compartment volume and surfaces, respectively. The ventilation flow contains the inevitable leakage flows as well.

Equation (1) is the central one to determine the pressure evolution as function of time. The expression explains why zone modeling can be successful: as long as the HRR and the heat losses, or, equivalently, the net heat gained/lost per unit time in the gas phase inside the enclosure, are known, the overall pressure evolution can be calculated without the need for detailed information on the flows inside the compartment.

Analytical approaches have been developed for the pressure evolution inside a compartment with natural ventilation through a single opening [12, 13]. A steady-state pressure value can be estimated from the fire HRR and the ventilation opening and relevant time scales can be defined, including the transport time inside the compartment and a pressure relaxation time [12]. The latter is indicative for the time it takes for the pressure to evolve (exponentially) to the steady state value. While this provides very valuable insight, the situation becomes far more complex when

mechanical ventilation is added, as illustrated by means of ‘electrical’ networks in [14]. It is considered worth exploring the analytical approach further in this respect.

However, in general, the flow field remains very relevant, particularly in fully predictive simulations, as the flow, combustion and resulting heat fluxes from flames, will determine the fire HRR evolution (and the evolution of the heat losses). Therefore, CFD has attracted attention in this context, in combination with HVAC (Heating, Ventilation and Air-Conditioning), e.g., [1, 2, 15, 16].

2.2. Energy balance

As mentioned, experimental data on the pressure evolution in case of fire in air-tight compartments with mechanical ventilation have been reported in [1-4, 7-9, 14, 17-21]. In [1, 2], results have been provided for tests with liquid fuel (heptane) and a polyurethane mattress, and also in [3] the fuel was liquid (hydrogenated tetra-propylene – HTP). In [7-9, 17, 18], experimental data, generated at UMons (Belgium), have been reported, using either wood cribs or liquid fuel (methanol). The use of liquid or solid fuel inevitably brings upon additional uncertainty, because the fuel mass loss rate, and thus the HRR, depends on the heat feedback from the flames and the compartment boundaries (see section 2.4). Therefore, Eq. (1) has been systematically further explored in experiments and numerical simulations in [14, 19-21], using gaseous fuel (propane) in an extensive experimental campaign in the NYX set-up at IRSN. Another difference between [14, 19-21] and [1-4, 7-9, 17, 18] is the size of the compartment: the NYX facility at IRSN in [14, 19-21] has a size of 1.25 m x 1.5 m x 1.0 m, while the studies in [1-4, 7-9, 17, 18] are at the size of a single or multiple rooms. The NYX set-up has been described in detail in [14, 19-21]. Fig. 1 shows a few images of what the flames looked like in one of the tests of [21].

All studies also mention the importance of the characterization of the leakage opening size and the ventilation network.



Fig. 1. Sequence of images during a NYX fire test of [21]. Pictures by H. Prêtre – IRSN. From top to bottom: ignition of pilot flame; ignition of fire source; steady combustion (3 pictures); decay phase; extinction.

From these studies, it has become clear that, notwithstanding very brief transient periods, the pressure evolution in an air-tight mechanically ventilated enclosure closely follows the RHS of Eq. (1), i.e., the net heat gained/lost per unit time in the gas phase in a qualitative manner [14, 19-21]. This is not necessarily what would be expected at first sight from Eq. (1), though, as the time derivative of pressure is on the LHS of the equation, not pressure itself. Fig. 2, showing the results of one test (Test I

in Table 1) in a systematic experimental campaign [20], reveals that the pressure itself, not the time derivative of pressure, follows the RHS of Eq. (1), particularly during the early stages [note that there is some uncertainty in estimating the heat losses from the compartment later on]. In these tests, using propane as gaseous fuel, the fire HRR was imposed according to the following expression:

$$\dot{m}_f = \begin{cases} 0 & 0 < t < t_1 \\ \alpha(t - t_1)^n & t_1 < t < t_2 \\ \dot{m}_{f,max} & t_2 < t < t_3 \\ \dot{m}_{f,max} - \alpha(t - t_3)^n & t_3 < t < t_4 \\ 0 & t > t_4 \end{cases} \quad (2)$$

where \dot{m}_f is the propane mass flow rate (g/s), α is the fuel mass flow growth/decay rate coefficient (g/sⁿ⁺¹), n is the flow growth exponent (-), $\dot{m}_{f,max}$ is the maximum (steady state) propane flow rate (g/s), $t_1 - t_2$ is the fire growth period (s), t_3 is the time to start decay (s), t_4 is the time when the fire goes out (s).

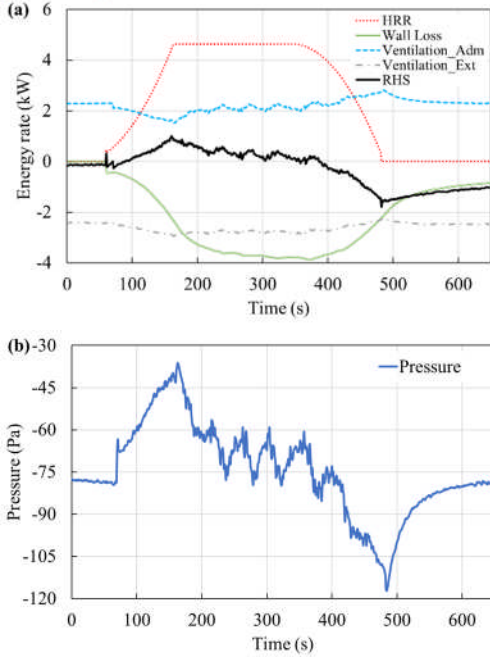


Fig. 2. Temporal evolutions of the energy terms (a) and the pressure (b) of Test I in Table 1 [20].

Table 1 Configurations of two fire test cases in the NYX set-up at IRSN [21]. Symbols refer to Eq. (2) for the imposed HRR.

Configurations	Test I	Test II
Name in the test campaign	F1A2	F1A4
α (g/s ³)	0.000005	0.01
$\dot{m}_{f,max}$ (g/s)	0.1	0.1
n	2	2
$t_2 - t_3$ (s)	180	180

This observation has been illustrated in, e.g., [17] (Fig. 12 in that reference), and the detailed discussion has been provided in [19]. The key equation reads (Eq. (18) in [19]):

$$\Delta p(t) - \Delta p_{init} \approx \frac{R_{eq}}{c_p T} (\dot{Q}_f - \dot{Q}_w) \quad (3)$$

In Eq. (3), $\Delta p(t)$ is the evolution of the relative pressure in the compartment, Δp_{init} is the initial value (with ventilation system active, prior to ignition of the fuel), R_{eq} is an equivalent flow resistance of the ventilation system (for details, see [19]) and T is the average temperature inside the compartment. Fig. 3 provides an illustration of this finding, showing the LHS and RHS of Eq. (3) as measured in the NYX set-up at IRSN.

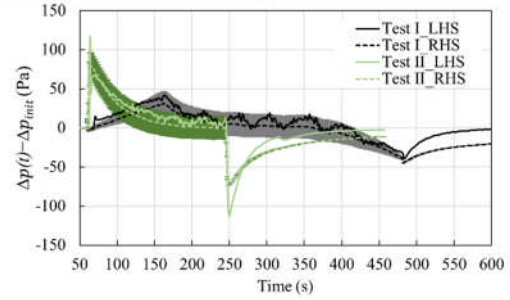


Fig. 3. LHS and RHS of Eq. (3) for the two tests of Table 1. The shadows indicate the uncertainty related to radiative heat loss calculations.

The key aspect is that the pressure directly affects the flows through the compartment boundaries (through leakage and/or mechanical ventilation) [19]. It is noted, though, that the relative importance of the time derivative of pressure will also depend on the ‘time constant’ of the problem, which pre-multiplies the time derivative: the larger this time scale, the more important the impact of the time derivative becomes. The time scale is proportional to the volume of the compartment and the flow resistance [19]. In CFD simulations all these aspects are accounted for automatically (if the boundary conditions are implemented in a proper manner). The use of a gaseous fuel, with direct control over the fuel mass flow rate (and hence the HRR) and potentially fast changes in HRR, is a strong advantage over solid or liquid fuels: fully controlled fast variations in HRR allow for a detailed analysis of the individual terms of Eq. (1) separately, because the other terms (heat losses in particular) cannot vary as quickly as the HRR.

From Eq. (1) and Eq. (2) it becomes clear that the HRR plays a very important role, as do the heat losses from the compartment. Before discussing these aspects in a bit more detail, some general findings from the studies mentioned are listed here. In [1, 2], it is concluded from a CFD study that the fire growth rate, the configuration of the dampers in the ventilation ductwork and the level of airtightness of the compartment have a strong impact

on the pressure evolution, while the activation or not of a roof-mounted fan had almost no impact. The latter is presumably due to the fan characteristics, in combination with the fire-induced pressure evolution. In [3] the conclusions are somewhat more precise and complete, in that there the overall HRR evolution (rather than the fire growth rate only) and the ventilation network in general (so not only the damper configuration) are mentioned to have a strong impact on the pressure evolution. Also, the importance of the thermal losses through the compartment boundaries and the geometry (volume of the compartment and the surface of the walls) are reported to have an impact on the pressure level. In [1-3] it is mentioned that a higher flow resistance leads to higher pressure peaks.

All of this is confirmed in [14, 19-21]. As mentioned, the use of propane allowed strong flexibility in terms of fire growth and decay (including the exponent of time, which needs not be quadratic), maximum steady state HRR and fire duration. Also, many different settings of the ventilation network have been tested, modifying the flow resistance in the admission and extraction duct, as well as the operation of supply and extraction fans. It was shown that the magnitudes of over-pressure and under-pressure peaks increase linearly with the maximum steady state HRR, and that for a given maximum steady state HRR, the magnitudes of the over-pressure and under-pressure peaks increase with increasing fire growth rate coefficient (until a plateau value is reached).

Given the importance of the HRR, for obvious reasons directly related to combustion phenomena, this is discussed in more detail in section 3.2.

2.3. *Flows through the compartment boundaries*

Although the term \dot{Q}_v in Eq. (1) can be very small, compared to \dot{Q}_f and \dot{Q}_w , it has been explained in [19] why the determination of the leakage opening size, and the flow resistance in general (in case of mechanical ventilation with ductwork) is essential for the absolute value of pressure (over-pressure and under-pressure). Eq. (15) of [19] shows that the pressure level is directly proportional to the 'equivalent' flow resistance, for given \dot{Q}_f and \dot{Q}_w . In other words, for given thermal conditions, the pressure varies less as the flow resistance becomes less (e.g., through larger openings).

Obviously, for simulations, and in particular CFD simulations, to be able to reproduce the pressure evolution accurately, it is essential to characterize the leakage opening size and the flow resistances and the fans as completely as possible. This is not straightforward, though. The leakage opening size is typically determined by means of a 'blower door test', with pressures up to 50 Pa. However, fire-induced pressures in air-tight compartments are much higher, so care must be taken as to how to extrapolate the data obtained [1, 2]. Some discussion is provided in [17] on this aspect. Also, the flow resistance is not always easy

to determine (and can vary when the gases are hot). In any case, it is essential to characterize the ventilation settings as completely as possible. The impact thereof on the pressure evolution has been discussed in detail in [14], where it was illustrated that, in addition to the well-known outcome of higher over-pressure and under-pressure peak levels for increased flow resistance in the ventilation system, not only the total, or 'equivalent', flow resistance is important, but also the individual flow resistances in the admission and extraction ducts separately. Indeed, the increase and reduction of ventilation flow rates depend on the fire-induced pressure, as well as the initial pressure difference in the ducts caused by flow resistance: flow rates vary more (respectively, less) strongly, depending on the pressure variation, as the flow resistance is lower (respectively, higher). The ratio between admission and extraction resistances leads to differences in flow variations in the admission and extraction ducts, hence potentially affecting the entire fire dynamics.

The discussion on the flow resistance characterization is not pursued here. It is only noted that leakage (among other phenomena such as, e.g., combustion) is a sub-grid scale phenomenon for CFD. In the CFD code FDS [22], e.g., this can be incorporated as bulk leakage or localized leakage, the latter obviously more relevant if the location of the leakage is known. The combination with an HVAC module, in order to allow for coupled compartment fire and mechanical ventilation simulations, is also available in FDS [14-16, 18-21]. More details can be found in [22].

2.4. *Heat losses through the compartment boundaries*

Eq. (1) makes clear that the heat losses into and through the compartment boundaries (\dot{Q}_w) play an important role in the pressure evolution. These heat losses are a combination of conduction in the solid material and heat exchange by convection and radiation with the gas phase. In general, modelling of convection in compartments will be challenging regardless of the approach used for estimating the convective fluxes (e.g., either due to the type of empirical correlation to use and/or due to the required grid resolution). Needless to say, it is important to characterize the material properties and heat fluxes as accurately as possible in experiments, and to fully describe the treatment in CFD simulations. It is noted that inevitably the heat exchange with the gas phase cannot be calculated as accurately in zone models as in CFD simulations (particularly if flame spread and preheating of virgin combustible materials would be involved). On the other hand, if the fire HRR (\dot{Q}_f) evolves (much) faster than the heat losses, the fire-induced over-pressure (due to fire growth) and under-pressure (due to fire decay) peaks are not necessarily affected strongly by \dot{Q}_w in case of mechanical ventilation (although temperatures inside the compartment obviously are affected directly) [21]. Indeed, \dot{Q}_w evolves towards \dot{Q}_f in equilibrium conditions (\dot{Q}_v being small in Eq. (1))

and hence is then determined by the HRR [19]. It remains to be explored how general this finding is, though. In any case, in periods where the HRR is steady, \dot{Q}_w has an impact on the transient pressure evolution.

As the characterization of the heat losses through the compartment boundaries is a heat transfer problem, not directly combustion related, the discussion is not pursued here.

2.5. Heat release rate

The HRR (\dot{Q}_f) evolution has been argued to play a central role. The treatment hereof in CFD simulations is discussed in section 3.2. However, the determination of the HRR is not straightforward in experiments, particularly when solid or liquid fuels are used, because then the HRR (considering the vaporization rate for liquid fuels and gasification rate for solid fuels) is to a large extent determined by the heat feedback from the flames and the compartment boundaries to the fuel. Moreover, the HRR cannot be measured directly. A classical approach, followed in, e.g., [1-4, 7-9] is to measure the mass loss rate of the liquid or solid fuel, using a load cell or alike. The mass loss rate itself is a sensitive quantity, as it is a time derivative of mass, the measurement of which has an accuracy that is determined by the accuracy of the weighing device. This is then multiplied by an ‘effective’ heat of combustion, i.e., the product of the theoretical heat of combustion and the combustion efficiency. For the latter there is also uncertainty, as this value is not necessarily constant during the test: in (locally) under-ventilated conditions, the effective heat of combustion is presumably lower than in well-ventilated conditions, and in case of solid fuel with char formation and variable heat feedback and oxygen supply (e.g., wood cribs) there is even less guarantee for a constant effective heat of combustion. Also, the determination of this effective heat of combustion is not straightforward (e.g., if blended and/or unknown fuels are present in a fire scenario). [In [1, 2], the HRR is reconstructed for the PU foam mattress fires through inverse modelling, based on temperature measurements, which is an even more indirect approach.]

As a consequence, a relatively large level of uncertainty is introduced, which makes it difficult to carefully validate numerical simulations at the level of pressure evolutions. An insightful paper on this is [23], comparing measurements based on oxygen consumption (OC) and carbon dioxide generation (CDG) for hydrocarbon pool fires in full-scale mechanically ventilated compartments. It is illustrated that modifications are necessary and that the CDG method is more appropriate in the given configuration, and that for both methods unsteady terms can have an important effect. It is concluded in [23] that ‘a confident estimation of the HRR’ requires appropriate measurements of flow rates, species concentrations, gas temperatures, soot concentrations and a ‘proper verification of mass balances in the compartment’.

The complexity of measuring the HRR accurately, was one motivation to use a gaseous fuel (propane) in the experiments of [14, 19-21]: setting the fuel mass flow rate with a flow controller makes it independent of heat feedback from the flames or the compartment boundaries, and as long as the conditions are well-ventilated, it is reasonable to assume that the effective heat of combustion is close to the theoretical value. Hence, a much more accurate value for the HRR can be assumed than in the case of liquid or solid fuels. An additional advantage is the full control over the HRR, and that fast variations of the HRR are possible, compared to solid or liquid fuel, allowing for more in-depth analysis of the individual terms in Eq. (1), as mentioned above. Hence, it is argued that future fundamental studies should consider using gaseous fuels if possible.

2.6. Scaling

Before addressing CFD, it is worthwhile to discuss how results would scale, depending on the geometry of the configuration. This will be particularly relevant when discussing amplitudes and frequencies of oscillatory behavior (section 4).

Reduced-scale experiments are popular in fire research due to the complexity and high costs involved in full-scale testing. Results are then scaled, based on physical scaling laws (e.g., [24-28]). The foundation, including the identification of the relevant dimensionless groups, was proposed in [29], and summarized and reported in more details specifically for reduced-scale fire modelling in [11, 24, 25]. It is reported that, given the central role of buoyancy in fire related flows, the Froude number is the primary number to preserve, whereas the Reynolds number is often not preserved [25, 30]. This implies partial or imperfect scaling and because the flows are normally turbulent in a full-scale fire, the size of the reduced-scale model must be sufficiently large to ensure turbulent flow (i.e., the Reynolds number must remain sufficiently high) [25]. To maintain the flow turbulence, it is mentioned in [25] that the height of the reduced-scale compartment should be at least 0.3 m.

A key parameter to preserve in scale modelling is the dimensionless HRR, as it is a dominant parameter affecting all fire-induced phenomena, as mentioned above. Full-scale fire scenarios of the PRISME tests [4] can be represented by, e.g., the NYX tests, through scaling up the HRR from the reduced-scale tests:

$$\dot{Q}_F = \dot{Q}_R \cdot \left(\frac{l_F}{l_R}\right)^{\frac{5}{2}} \quad (4)$$

where \dot{Q}_F and \dot{Q}_R are the heat release rate of the full-scale and reduced-scale, respectively. For the NYX compartment, the geometric scale ratio $l_F/l_R=4$ when compared to the full-scale PRISME tests [31].

In doing so, time should be scaled as a function of the length scale as well [25]:

$$t \propto l^{\frac{1}{2}} \quad (5)$$

It is noted that a specific difficulty in scaling fires relates to the heat transfer. In the reasoning above, the temperatures in the reduced-scale experiments are supposed to be identical to the ones at full scale. Yet, this does not guarantee identical heat transfer from the gas phase (soot formation may be different, leading to differences in radiation, and the change in the turbulence level may affect the convection coefficient). In addition, it is not straightforward to scale the heat transfer by conduction into the solid, as the thermal penetration depth varies with time, which by itself is supposed to scale. These are important issues to address when studying the pressure evolution in the air-tight compartment [24]. Fig. 4 shows that the conductive heat fraction (conduction/HRR) at full-scale is somewhat smaller than that at reduced-scale. This is in line with the conclusion in [32], stressing the importance of scaling the heat transfer through the walls in a confined compartment.

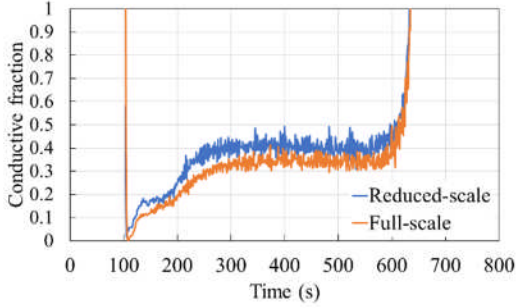


Fig. 4. Relative contribution of the conductive heat losses (expressed as the ratio to the HRR) as obtained in CFD simulations for different scales.

It is also stressed in [32] that the global equivalence ratio (GER) should be conserved in scaling of mechanically ventilated confined compartments, so as not to affect the combustion regime inside the compartment (see also section 4.2 below). This determines in particular the scaling of the ventilation flow rate.

However, another aspect concerns transient pressure phenomena. This can be made clear when pressure scaling is analysed from the perspective of energy balance, more specifically, the energy balance of Eq. (11) in [19] (see Eq. (6) here) and the elaborated form of Eq. (16) in [19] (see Eq. (7) here):

$$\begin{aligned} \frac{V}{\gamma - 1} \frac{d}{dt} \Delta p(t) + \frac{\Delta p(t)}{R_{flow,adm}} c_p T_{adm} + \frac{\Delta p(t)}{R_{flow,ext}} c_p T_{ext} \\ + \frac{\Delta p(t)}{R_{flow,leak}} c_p T_{leak} = \dot{Q}_f - \dot{Q}_w \\ + \frac{\Delta p_{AF}(t)}{R_{flow,adm}} c_p T_{adm} - \frac{\Delta p_{EF}(t)}{R_{flow,ext}} c_p T_{ext} \end{aligned} \quad (6)$$

$$\Delta p(t) \approx \frac{1}{c_p T} R_{eq} \left(\dot{Q}_f - \dot{Q}_w + \frac{\Delta p_{AF}(t)}{R_{flow,adm}} c_p T - \frac{\Delta p_{EF}(t)}{R_{flow,ext}} c_p T \right) \quad (7)$$

The scaling results of each term in the energy balance of Eq. (7) indicate that if the pressure scales

as proportional to l , everything is consistent [21]. For Eq. (6), however, the same elaboration reveals an inconsistency for the first term on the left-hand side, which scales as $p l^{\frac{5}{2}}$, while all other terms in Eq. (6) scale as either $p l^{\frac{3}{2}}$ or $l^{\frac{5}{2}}$ (so that the scaling would still be fine for all terms but the first one on the LHS if $p \propto l$). This inconsistency is not seen in Eq. (7) because the first term on the left-hand side of Eq. (6) is assumed negligible in the reasoning leading to Eq. (7). This assumption may not be true when the pressure rises very rapidly. Therefore, a case with fast pressure rise, namely Test F3A23 (i.e., Test CIV in [19]), has been analysed by means of CFD simulations with FDS, version 6.7.5 [33], to evaluate if the pressure scales as l or not. Two sets of CFD simulations have been performed, with the correct scaled-up parameters as listed in Table 2 (where t_{growth} is the time it takes for the HRR to evolve from 0 to the maximum value).

The comparison between reduced-scale and full-scale pressure variations in Test F3A23, for the given imposed HRR evolution, is shown in Fig. 5 (moving averages, using 15 consecutive data points in time, are shown in order to remove fluctuations from the figures, so that the evolution is seen more clearly). The line ‘Full-scale’ has been retrieved directly from the CFD simulations, while the line ‘Reduced-scale $\times 4$ ’ is the result from the reduced-scale CFD results, multiplied by 4. As mentioned above (Eq. (6)), time (i.e., horizontal axis) has been scaled as $l^{1/2}$ for the reduced-scale results.

During the periods of steep variations in HRR, and hence induced pressure, some discrepancies are observed between p_F and $p_R \times l$. Zoom-in plots for the over-pressure and under-pressure periods are shown in Fig. 6. For the periods where the pressure increases/decreases rapidly, there are discrepancies between full-scale and amplified reduced-scale results and there is a delay for the full-scale pressure to reach the peak value. The transient phenomenon is slower, because the term is pre-multiplied by $l^{\frac{5}{2}}$ (and not $l^{\frac{3}{2}}$), so that at larger scale the time derivative should be lower to compensate for the larger pre-multiplicator in the balance equation. Nevertheless, the order of magnitude between the full-scale and the amplified reduced-scale results is comparable and overall the pressure is observed to scale reasonably as proportional to l , confirming the above. The pressure level in the full-scale simulations is somewhat higher. This is in line with Fig. 4, where it was illustrated that the conductive heat losses are relatively higher at reduced-scale (using the same materials).

Table 2. Scaled-up parameters of the fire corresponding to the reduced-scale Test F3A23 [21].

Scale	$\dot{m}_{f,max}$ (g/s)	n	α (g/s ²)	t_{growth} (s)	$\dot{Q}_{f,max}$ (kW)
Reduced-scale	0.35	1	1	0.35	16.20 5

Full-scale	11.2	1	16	0.7	518.5
					6

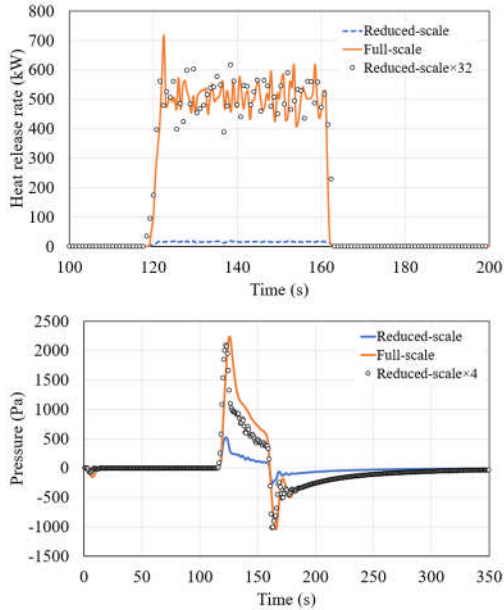


Fig. 5. Comparison between reduced-scale and full-scale moving average temporal evolution of pressure variations in Test F3A23 (bottom figure). The hollow dots indicate the theoretical scaled-up pressure (i.e., scaled proportional to the length scale). Top figure: evolution of the HRR. Note that the time (i.e., horizontal axis) has been scaled as $l^{1/2}$ for the reduced-scale results.

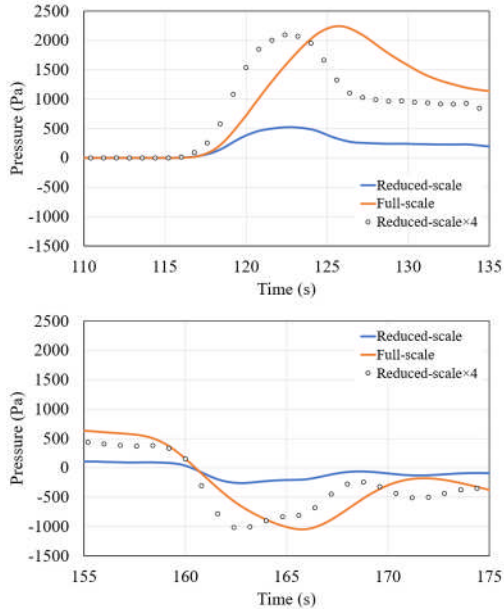


Fig. 6. Zoom-in of the comparison between reduced-scale and full-scale moving average temporal evolution of pressure variations in Test F3A23 (see Fig. 5). Top: 110 s – 135 s; Bottom: 155 s – 175 s.

3. Turbulent combustion in CFD simulations of compartment fires

3.1. General discussion

A good overview of state-of-the-art CFD approaches in fire simulations is found on [34], the database for the IAFSS Working Group ‘MaCFP’ (Measurements and Computations of Fire Phenomena) [35].

The common approach for turbulence is Large Eddy Simulations (LES), so that large-scale unsteadiness is captured. This is the case in FDS [22], with a choice for subgrid-scale models (details found on [22]), and in FireFOAM [36], another widely used CFD package for fire safety science and engineering research. Although not yet commonly used, a dynamic approach for the modelling of turbulence, combustion and (simplified) radiation seems worth exploring in the context of fully predictive fire simulations [37, 38]. This is not discussed further here, as the focus is on the HRR.

In fire simulations, a common approach to model turbulent combustion is the use of infinitely fast chemistry, combined with a version of the Eddy Dissipation Model/Concept (EDM/EDC) [39] to account for turbulence-chemistry interactions, but mixture fraction-based approaches are also possible, see below. This, however, can have an impact on the HRR inside the computational domain, as discussed in section 3.2.2.

3.2. Heat release rate

3.2.1. Evaporation/pyrolysis

The uncertainties related to the HRR when using a liquid or solid fuel in experiments have been mentioned in section 2.4. In CFD simulations, the use of a liquid or solid fuel also adds significant complexity and uncertainty. Indeed, flaming combustion occurs in the gas phase and hence the model for evaporation (liquid fuel) or pyrolysis (solid fuel) has a strong impact on the results, as this model, in combination with the local heat balance, determines the fuel mass flow rate into the gas phase (and hence to a large extent the HRR). The positive feedback loop in this process makes everything even more sensitive. The development of evaporation and pyrolysis models is a lively research area, but this is considered beyond the scope of the present paper.

3.2.2. Gaseous fuels, well-ventilated conditions

As mentioned above, the EDM/EDC approach [39] is popular in CFD simulations for fires (where non-premixed combustion is often the dominant mode). There are many variants, but the key aspect of relevance in the discussion of the HRR is that the method works directly on the CFD mesh, with the (local) mass loss rate of the fuel (or oxidizer) directly present as source term in the transport equation for fuel (or oxidizer) mass fraction, and upon multiplication with the heat of combustion, directly present as source term in the transport equation for sensible enthalpy or temperature [22,

36]. This implies that if the entire mass flow rate of fuel that enters the computational domain burns completely inside the computational domain, the total HRR as released automatically matches the injected value. [Whereas this may seem a trivial statement, this is not straightforward for mixture fraction based turbulent combustion modelling for fire flames, as discussed below.] Reduced HRR values inside the computational domain then indicates incomplete combustion and this can then effectively be used to quantify the overall extinction level. A major disadvantage, though, is that the rate of combustion is entirely determined by the fuel-air mixing rate, and hence no combustion chemistry kinetics is taken into account. The latter can be relevant for extinction / re-ignition phenomena (see section 3.2.3).

This motivated research studies with renewed interest in mixture fraction-based combustion models, previously used with RANS turbulence modelling (e.g., [40]), now combined with LES [41-47]. In these mixture fraction-based models, the HRR is essentially determined in mixture fraction space. In [41, 42] an equilibrium between chemistry and diffusion is assumed, so also gradients in physical space are used, but in the end the HRR is calculated from mixture fraction space, multiplying the reaction rates of species mass fractions with their heats of formation (which is equivalent to the use of a heat of combustion). In [43], in addition to results with EDC, the steady laminar flamelet model [48, 49] is applied. The look-up tables are constructed with mixture fraction, conditional scalar dissipation rate (CSDR) at stoichiometric conditions and enthalpy deficit as independent variables. The latter intends to account for radiative losses and two methods are compared in [43] (but that discussion is considered beyond the scope of the present paper). In [44, 50] it is argued that unsteady effects are important for accurate radiation modelling due to the low values of scalar dissipation rate in the buoyancy-driven flames that are typical in fires: the mixing rates of fuel and oxidizer are slow, leading to long response times of the flames; and at low flame stretch rates, the flames become physically and optically thicker. The latter reflects that radiation becomes relatively more important in fire flames, compared to jet flames (not mentioning the presence of soot) [44, 50]. Therefore, the unsteady laminar flamelet (ULFM) approach [51], more particularly FlameMaster [52], has been used to include this. The tables are again constructed with mixture fraction, CSDR at stoichiometric conditions and enthalpy deficit as independent variables. An 'effective' CSDR is introduced, as discussed below. In [45], the conditional moment closure (CMC) method [53] is applied, using the CMC code as developed at the University of Cambridge [52]. The spatial transport terms in the CMC equations, which make the difference from the ULFM approach, are shown to have an impact when radiation is included in the simulations (as should always be the case in fire simulations), but more importantly the findings in [45] on the importance of the CSDR are very much in agreement with the discussion in [44]. This

is also in line with the findings in [54]: the CSDR – not only the value at stoichiometric conditions, but the shape in the entire mixture fraction space - is extremely important for radiation in mixture fraction based turbulent combustion modelling with finite rate chemistry in fire related flames.

From the above, and not unlike for jet flames, it is clear that the CSDR is a key quantity in mixture fraction based turbulent combustion models for fire flames. What is specific for the latter, though, is that the values for CSDR are significantly lower than in jet type flames. As explained in [44], this brings upon the issue of long response times of fire flames, while subjected to rapidly changing local conditions due to turbulence. Consequently, relaxation to quasi-steady conditions is not possible [44]. This brings upon the concept of an 'effective' CSDR, based upon the idea of the 'equivalent' strain rate, taking into account history effects, as introduced in [55]. This equivalent strain rate incorporates unsteadiness effects into a steady LFM framework, and the reasoning has been applied in [44], using the ULFM approach: it is argued that the effective CSDR, rather than the local CSDR, is much more representative as parameter to describe the mixing of fuel and oxidizer in diffusion flames in an unsteady environment, and hence should be used to determine the local response of a fire flame. In [45] the concept of effective CSDR is not used, but it is worth exploring how that concept would affect the CMC results.

It is noted that mixture fraction-based modelling relies on a chemistry mechanism to provide the link between mixture fraction (and other independent variables as mentioned) and the species mass fractions and temperature, while in fires often the fuel combustion chemistry is not well-known. Often the fuel itself is not well-characterized and then this shortcoming prevails a fortiori. This is a point of attention when using mixture fraction-based models in the context of fire.

As a final important note, it is repeated that with mixture fraction-based combustion models, the HRR is essentially determined in mixture fraction space. As a consequence, even in the case of complete combustion of the fuel within the computational domain, the integrated value of the HRR is not necessarily identical to the injected value at the inlet boundary of the computational domain, as explicitly mentioned in [44, 45]. The reasons can be multiple, including details on the (assumed) PDF (shape), integration of the PDF, numerical accuracy and others. Unfortunately, this is not necessarily noticed in the analysis of the CFD simulations, if the HRR is not used directly: in [40, 43-47] no equation for temperature (or sensible enthalpy) is solved on the CFD mesh; in [41, 42] the transport equation for temperature is solved, but given the overall uncertainty (e.g., related to radiation or soot) the results for temperature do not allow to assess whether the integrated HRR is equal to the injected value. A detailed systematic investigation of the integrated HRR within the computational domain with mixture fraction-based models is therefore argued to be a relevant research task for the near future, particularly if the local

HRR is used in modeling (e.g., radiation modeling) or if the integrated HRR value is to be used to quantify levels of incomplete combustion / extinction. In the context of fire-induced pressure in mechanically ventilated compartments, the HRR is also key, as argued before, stressing the importance of the suggested research. The use of such models in numerical simulations of mechanically ventilated compartments has the potential to predict minor species and/or flame extinction more accurately than simplified models based on infinitely fast chemistry.

3.2.3. Extinction and re-ignition

As mentioned in section 3.1, the EDM/EDC approach is commonly used in CFD simulations of fires. A major advantage is its relative simplicity and limited computational cost, while accounting for the impact of turbulence on the reaction rates. As explained in section 3.2.2, also the integrated HRR is captured well automatically. In its simplest formulation, and this is the most widely approach as used today in state-of-the-art fire simulations [34], infinitely fast chemistry is assumed.

A disadvantage of this ‘mixed-is-burnt’ approach, particularly in under-ventilated conditions, is that an additional model is required to incorporate extinction and re-ignition. This is particularly relevant in the context of fire simulations in air-tight compartments, as, depending on the oxygen supply, the conditions can vary from fuel-controlled to ventilation-controlled (or even alternate between the two, as discussed in section 4). Needless to say, extinction and ignition phenomena occur at scales that are not resolved on a CFD mesh (i.e., they are considered sub-grid scale effects) for fire simulations and hence require modelling.

An interesting asymptotic analysis of local extinction in diffusion flames, relevant for fires, is provided in [56]. This ‘activation energy asymptotic’ (AEA) approach was elaborated in [57], leading to the well-known S-shaped curve, in the context of an irreversible 1-step chemical reaction of fuel and oxidizer with high activation energy. This leads to a single Damköhler number criterion that allows to describe different types of extinction of non-premixed flames, labeled in [56] as ‘aerodynamic’, ‘thermal’ and ‘dilution’ quenching. The Damköhler number compares a mixing (or flow) time scale to a chemical time scale, and, when considering only the effect of temperature on the chemical kinetics, can be defined as:

$$Da = \frac{\tau_{mix}}{\tau_{chem}} \propto \frac{1/\chi_{st}}{\exp\left(\frac{T_a}{T}\right)} \quad (8)$$

In this expression, an Arrhenius expression is assumed for the chemical kinetics (note that the pre-exponential factor, with unit s^{-1} , has been removed in the denominator), with T the flame temperature and T_a the activation temperature. In the numerator, χ_{st} is the CSDR (see section 3.2.2) at

stoichiometric conditions, assumed to be representative for the local mixing rate of fuel and oxidizer at the flame. Aerodynamic quenching occurs when the CSDR becomes high, while thermal quenching (due to heat losses, such as radiation) and dilution quenching (due to air or fuel vitiation) happens when the local temperature becomes too low (and hence the chemical time scale increases). When the Damköhler number drops below a critical value, the flame extinguishes. As mentioned in section 3.2.2, the CSDR values in buoyancy-driven flames, typical for fires, are usually relatively low, so aerodynamic quenching is not the typical mechanism for fires. This is reflected in the modelling, as discussed next. An example of the flammability map for methane-air diffusion flames implied by the Damköhler number-based flame extinction models given by Eq. (8) is presented in Fig. 7. In this case, flame extinction occurs for large values of flame stretch and low values of flame temperature. Typically, large values of flame stretch are associated with high turbulence intensities while low values of flame temperature result from oxygen dilution effects and/or thermal losses [58].

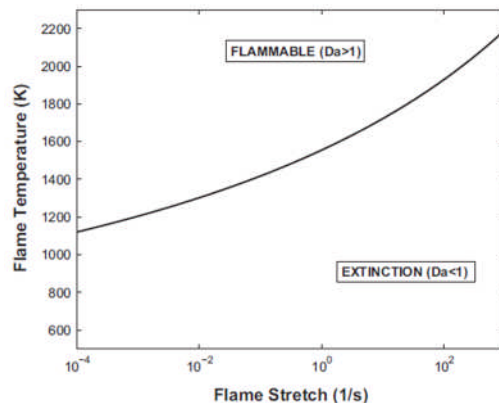


Fig. 7. Flammability map for methane-air diffusion flames using flame stretch, χ_{st} , and flame temperature, T , as coordinates. The solid black line corresponds to the extinction limit, $Da_{crit} = 1$. Figure reproduced from [58].

In FDS [22], rather than using the concept of the critical Damköhler number, extinction is modelled on the basis of a critical flame temperature (CFT), also using a limiting oxygen index (LOI): if the potential heat release by combustion inside a CFD cell cannot raise its temperature above the CFT (considering an enthalpy balance), the reaction is suppressed. [Note that there is also an extinction model, based on oxygen concentration mainly, for coarse grids [22].] This approach was introduced in [59]. Focusing on temperature (or heat) only, the CFT based extinction model refers to thermal quenching only, not considering aerodynamic or kinetic quenching. This may be justified in fire flames that exhibit low strain rates and had been confirmed in the simulations of [60], comparing CFT based to the critical Damköhler based

extinction modelling of [58]. The latter takes into account chemical time scales, compared to flow time scales, and hence can cover aerodynamic quenching in principle, but the results are very similar to the CFT based results, in line with the fact that the thermal quenching mechanism is dominant.

It is worth noting that the combined modelling of turbulence, combustion, radiation (and thus also soot modelling, depending on the fuel involved) and flame extinction/re-ignition modelling, has a direct influence on the predicted temperatures, hence, also in the evaluation of the enthalpy balance. Dissipative turbulence models could result in a more laminar-like flame; simplified combustion models based on infinitely fast chemistry might not accurately predict CO₂, H₂O and minor species; and over/under predictions of the radiative fractions depending on the radiation modelling approach will directly influence the resulting flame temperatures. Adding the need to have accurate predictions over a wide range of grid sizes poses an additional requirement for CFD codes and the employed models. In fact, these aspects often pose some limitations in the application of the employed approach for modelling flame extinction in scenarios where coarse grids are employed (e.g., due to limited computational resources).

Another approach towards extinction, in the spirit of the fact that the reaction zone, and hence the extinction phenomenon, is not resolved on the CFD mesh, builds upon the concept of ‘fine structures’, using a perfectly stirred reactor (PSR) assumption [61-63]. The reaction zone is then treated as a PSR, to which fuel and oxidizer are supplied. The temperatures and compositions are determined by the locally resolved cell values and the mixing rate is determined by the local turbulence. Not unlike the AEA approach, also the PSR based extinction modeling results in a critical Damköhler number, below which extinction is supposed to occur. Hence, aerodynamic, thermal and dilution quenching are covered (the former called ‘blow-off’ in [62]). An advantage of the PSR approach is that the activation energy need not be high, which can be relevant in vitiated conditions [62]. It is also noted that there is no need to formally distinguish between non-premixed and premixed flames. Within the context of a single-step global combustion reaction, kinetic parameters have been determined in [62] on the basis of measured flame temperatures and strain rates for blow-off conditions (aerodynamic quenching). In order to cover thermal quenching (i.e., extinction due to thermal losses, despite long enough residence times for fuel and oxidizer to mix and react), the model of [62] has been extended in [63] to account for radiative losses, with an optically thin assumption. The model becomes more complex, but covers the different forms of extinction, defining a critical Damköhler number based on the inverse of the strain rate as residence (flow/mixing) time scale, and the chemical reaction rate time scale determined from an Arrhenius expression, such that fuel dilution (through mass fractions) and thermal losses (included in the calculation of the flame

temperature) are taken into account. It is explained in [63] how this can be implemented as a sub-grid scale model in LES simulations.

While extinction modelling is important, the necessity of avoiding spurious re-ignition is emphasized in [58, 60]. This concerns unrealistic ignition of fuel – oxidizer mixtures within the flammability limits, but at too low of a temperature to ignite in reality. In [60] two suggestions are formulated, namely a re-ignition criterion based on a critical temperature (but this has the disadvantage of also eliminating desired ignition, when applied to the entire computational domain), or the introduction of a tiered reaction mechanism, effectively separating ignition and re-ignition. While there is some degree of arbitrariness in the choice of critical temperatures, this is an appealing engineering approach. Accurate modelling of combustion (i.e., in terms of resulting mean and rms flame temperatures) and radiation (i.e., in terms of predicted radiative fractions), along with relatively small grid sizes, is a pre-requisite for accurately predicting flame extinction. The choice of a simple re-ignition model, based on a constant re-ignition temperature, can be as important as the flame extinction model itself when infinitely fast chemistry is assumed. Hence, there is need for more advanced re-ignition models which also include the local composition and strain rate. A theoretical framework has been elaborated in [64] for quenching and re-ignition of ‘mixed eddies’, i.e., regions in turbulent non-premixed flame zones where fuel, oxidizer and combustion products are mixed. The composition, size and temperature determine whether a mixed eddy will be quenched or re-ignited, considering the heat released per unit time by chemical reaction (for which a one-step Arrhenius reaction is assumed in [64]), as well as the heat lost per unit time by conduction and radiation [64]. This in the end leads to the use of the turbulent Karlovitz number to determine quenching and re-ignition, and an effective turbulent reaction rate in [62]. In general, re-ignition modelling is arguably important, in particular in the context of under-ventilated compartment fires (see also section 4), and hence deserves more research. Re-ignition modelling becomes particularly important when infinitely fast chemistry is considered since the evaluation of the re-ignition criterion strongly depends on the predicted flame temperatures which are highly affected by the grid resolution.

It is recalled that, as mentioned in section 3.2.2, inclusion of detailed finite rate chemistry mechanisms, be it within the EDC framework or with mixture fraction-based combustion models, should have the potential of automatically predicting extinction and (re-)ignition. Within the context of fires, though, the fuel and detailed chemistry are often not known, so it is questionable to date whether this is a viable approach in fire simulations. Yet, this deserves to be explored in the future and could be useful to generate numerical databases against which the models mentioned above can be tested. In the same view, transported PDF/FDF modeling [65] is worth investigating in the context of fire simulations.

Finally, it is noted that, given the importance of thermal quenching in fire simulations, also radiation is key. This involves soot as well, particularly if the radiative fractions are predicted or prescribed in the modelling. In the former case, prediction of flame extinction as a function of grid size can be quite challenging [60, 66]. In turn, this should have a direct impact on the evolution of the HRR, which is of particular importance for fires in air-tight compartments, as discussed above. All of these are very lively research areas, both in terms of experiments and numerical simulations, and it is argued that more in-depth understanding and insights should link to further development and validation of extinction and reignition models as well, important for accurate estimates of the HRR as function of time (and hence important for the pressure evolutions, as shown in Eq. (1)).

3.3. Dynamic modelling

Modelling in CFD for fires has relied, to some extent, on turbulence models and combustion models with model parameters that have been derived for highly turbulent flows, conditions that are not necessarily representative of the ones encountered in turbulent buoyant fires. The use of dynamic models can help overcome such deficiencies but has not (yet) become the standard practice in fire modelling. The wide range of time and length scales, often encountered in typical fire scenarios, poses a significant problem in the application of such models mainly due to their increased computational cost. Nevertheless, the ever-increasing growth in hardware and software capabilities seen in computer science during the past decades, has allowed more detailed and well-resolved CFD simulations for a wide range of engineering applications. It is expected that the use of dynamic modelling will be more feasible than ever in the near future, also for numerical simulations of (large-scale) fire applications.

3.3.1. Turbulence modelling

The conceptual mathematical framework of dynamic turbulence modeling is double filtering [67]. In principle, the predictive capabilities of such dynamic turbulence models could be assumed to be potentially superior, compared to models using constant coefficients. Particularly when it comes to fire modelling, their advantages are multifold. Firstly, the laminar to turbulence transition, a key characteristic of all pool fires, can be captured without the need of tuning/adjusting the turbulence model parameters [38, 68]. Secondly, the sub-grid scale viscosity and kinetic energy evolve towards zero near walls without the explicit need for damping functions [69], which is a particularly important feature as most fire scenarios involve either enclosures and direct interaction with surfaces. The latter is particularly critical in the context of fully coupled gas/liquid or gas/solid fire simulations. Thirdly, the predicted sub-grid scale (sgs) viscosity and kinetic energy do not explicitly depend on the grid size, as the filter width is eliminated through the dynamic procedure (e.g., in

the dynamic Smagorinsky when calculating c_s for sgs viscosity and c_l for sgs kinetic energy) and the ratio of the test filter to grid size is more relevant. Nevertheless, the filter width is still present in the calculation of the model parameters (e.g., c_s and c_l). Finally, dynamic models will correctly tend towards zero sub-grid scale viscosity and kinetic energy as the DNS limit is reached.

Nevertheless, the dynamic models do also have their disadvantages, namely that they are computationally more expensive and they can lead to oscillations and/or perform poorly on relatively coarse grids. The latter aspect is particularly important if these models are to be used for CFD of engineering purposes.

The widely-known dynamic Smagorinsky model for modelling turbulence has been adopted in [37, 38]. The sub-grid scale viscosity is calculated as:

$$\mu_{sgs} = \bar{\rho}(c_s\Delta)^2|\tilde{S}| \quad (9)$$

where Δ is the filter width (taken as the cube root of the cell volume) and S is the (resolved) strain rate. The dynamic procedure does not allow the model parameter c_s to take negative values while no upper bound is defined.

The sub-grid scale kinetic energy is estimated as:

$$k_{sgs} = c_l\Delta^2|\tilde{S}|^2 \quad (10)$$

with the model parameter c_l (as well as c_s) computed dynamically as local averages, using their values on the cell faces.

The sub-grid scale dissipation rate is modelled as:

$$\varepsilon_{sgs} = \frac{c_\varepsilon k_{sgs}^{\frac{3}{2}}}{\Delta} \quad (11)$$

where $c_\varepsilon = 1$ [38] is a model constant.

The sub-grid scale thermal diffusivity is calculated as $\alpha_{sgs} = \mu_{sgs}/\rho Pr_t$ with the turbulent Prandtl number, Pr_t , determined from a dynamic procedure [37, 38]. The turbulent Schmidt can also be calculated dynamically, or can be set to $Sc_t = Pr_t$.

Recently [38], the predicted turbulence model parameters related to sub-grid scale viscosity and kinetic energy, determined based on a dynamic procedure, were found to be significantly lower in all the plume scenarios examined, compared to their theoretical values obtained from homogeneous isotropic decaying turbulence. More specifically, the resulting turbulence modelling parameters in the near-field region of the fire plumes were found to range between $c_s \approx 0 - 0.1$, $c_l \approx 0.05 - 0.15$ and $Pr_t \approx 0.1 - 0.5$. The resulting average turbulence modelling parameters in the far-field region of the fire plumes were found to be in the order of $c_s \approx 0.1$, $c_l \approx 0.15$ and $Pr_t \approx 0.5$. Nevertheless, significant variations around these values were evident depending on the location examined and the dynamic procedure was able to capture them to some extent. The work

demonstrated the potential of using dynamic modelling approaches in order to enhance predictive fire modelling. Yet, further evaluation of these dynamic turbulence models in more challenging fire scenarios involving, e.g., flame spread and pyrolysis, is required in the future. This is suggested as a route for further research.

It is noted that the (dynamic) Smagorinsky model is not the only option in fire simulations. In FDS, e.g., the default turbulence modelling approach for LES is a modified version of the Deardorff model [70], where the sub-grid scale kinetic energy is taken from an algebraic relationship based on the scale-similarity model of [71]. The turbulent Prandtl and Schmidt numbers are typically assumed constant, while the WALE model of [72] is applied to calculate the SGS viscosity in the first off-wall grid cell.

3.3.2. Turbulent combustion

As mentioned in section 3.2, a widely-used combustion model for combustion applications is the Eddy Dissipation Concept (EDC), particularly due to its simplicity and its capabilities to incorporate finite rate chemistry effects. The use of the model for fire applications has, until now in the literature, been limited to considering infinitely fast chemistry (hence not attempting to predict minor species).

A formulation of the EDC model [73] where the model parameters, C_γ and C_τ , are not constants but vary dynamically, previously applied for combustion modelling of pool fires [37], is presented below.

According to the energy cascade theory, the largest energy-containing eddies are highly unstable and break down into smaller eddies until they are sufficiently small (i.e., have the size of the Kolmogorov length scale) and they are dissipated into heat. Within EDC, these small eddies are called fine structures and such regions can be treated as, e.g., Perfectly Stirred Reactors (PSR) in which chemical reactions depend on the molecular mixing between the reactants. These fine structures are intermittently distributed and only a fraction of them can react. By considering a one-step, infinitely fast, chemical reaction, the fuel reaction rate is calculated as:

$$\overline{\dot{\omega}_F'''} = \bar{\rho} \frac{\gamma^2 \chi}{\tau(1 - \gamma^3 \chi)} \min\left(\frac{\tilde{Y}_F}{s}, \frac{\tilde{Y}_{O_2}}{s}\right) \quad (12)$$

where γ is the size of the fine structures, τ is the mixing time scale, χ is the reactive part of the fine structures, s is the oxygen-fuel mass stoichiometric ratio while \tilde{Y}_F and \tilde{Y}_{O_2} are the filtered mass fractions of fuel and oxygen, respectively.

The size of the fine structures can be expressed as:

$$\gamma = C_\gamma \left(\frac{\nu \varepsilon_{sgs}}{k_{sgs}^2}\right)^{\frac{1}{4}} \quad (13)$$

with $\gamma < 1$ and C_γ a model parameter calculated as:

$$C_\gamma = Da_\eta^{\frac{1}{2}} (Re_T + 1)^{\frac{1}{2}} \quad (14)$$

with Da_η the Damköhler number, evaluated at Kolmogorov scale, and Re_T the turbulent Reynolds number.

For infinitely fast chemistry, χ is calculated as:

$$\chi = \begin{cases} \frac{s\tilde{Y}_{ref} + Y_{O_2}^0}{Y_{O_2}^0}, & \text{if } \tilde{Y}_{ref} < 0 \\ \frac{Y_F^0 - \tilde{Y}_{ref}}{Y_F^0}, & \text{if } \tilde{Y}_{ref} \geq 0 \end{cases} \quad (15)$$

where Y_F^0 is the initial fuel mass fraction in the fuel stream, $Y_{O_2}^0$ is the initial oxygen mass fraction in the oxidizer stream and $\tilde{Y}_{ref} = \tilde{Y}_F - \tilde{Y}_{O_2}/s$.

The estimation of the mixing time scale is modified compared to the origin formulation of the model as:

$$\tau = \min(\tau_{turb}, \tau_{lam}) \quad (16)$$

which effectively considers mixing under turbulent and laminar conditions. The turbulent time scale is based on the original energy cascade model taken as the Kolmogorov time scale:

$$\tau_{turb} = C_\tau \left(\frac{\nu}{\varepsilon_{sgs}}\right)^{0.5} \quad (17)$$

where C_τ is model parameter calculated as:

$$C_\tau = \frac{1}{Da_\eta (Re_T + 1)} \quad (18)$$

while the laminar time scale is estimated as:

$$\tau_{lam} = \frac{\Delta^2}{C_{diff}\alpha} \quad (19)$$

where $C_{diff} = 4$ [37] is a model constant.

The Damköhler number, comparing the molecular mixing process at the Kolmogorov scale to the reaction in the fine structures, is evaluated as $Da_\eta = \tau_\eta/\tau_c$ where $\tau_\eta = (\nu/\varepsilon_{sgs})^{0.5}$ is the Kolmogorov time scale. The characteristic chemical time scale is evaluated by considering an Arrhenius equation as $\tau_c = Ae^{-T_A/T}$ where the pre-exponential factor, A , and the activation temperature, T_A , are taken from a global one-step reaction mechanism for the fuel considered. The turbulent Reynolds number is calculated based on the sub-grid scale kinetic energy and dissipation rate as $Re_T = k_{sgs}^2/(\nu\varepsilon_{sgs})$. In regions where Re_T becomes low (i.e., laminar conditions), the calculation of the fuel reaction rate can become problematic: it can increase drastically and can potentially lead to unphysical behavior. To prevent

this problem, the ratio $(\gamma^2\chi)/(1 - \gamma^3\chi)$ is clipped to values ≤ 1 .

It is important to mention that the existence of an inertial sub-range in the turbulence energy spectrum is not at all guaranteed in fires. Also, relatively coarse meshes are used quite commonly in fire simulations. In that light, it is worth mentioning that in FDS, based on [74], the time scale (Eq. (16)) has been adjusted, taking into account buoyancy:

$$\tau_{mix} = \max\left(\tau_{chem}, \min(\tau_d, \tau_u, \tau_g, \tau_{flame})\right) \quad (20)$$

where the chemical time scale ($\tau_{chem} = D_F/s_l^2$), with D_F the fuel mass diffusivity and s_l the laminar flame speed, is compared to: the mixing time for diffusion ($\tau_d = \Delta^2/D_F$); sub-grid scale advection ($\tau_u = C_u\Delta/\sqrt{(2/3)k_{sgs}}$); buoyant acceleration ($\tau_g = \sqrt{2\Delta/g}$); and an upper limit on very coarse meshes (τ_{flame}). This reaction time scale model proposes a scaling regime for coarse mesh resolution based on buoyant acceleration. As explained in [74], for fires which are generally buoyancy-driven flows, buoyant acceleration is expected to control the mixing at relatively coarse scales. Hence, a time scale based on a constant acceleration that scales with the square root of the filter width is proposed. Both τ_{chem} and τ_{flame} effectively pose the extreme limits that τ_{mix} can take in the reaction time scale model.

In the context of SGS coupled advection-diffusion-reaction, the Linear Eddy Model of [75] may also be worth exploring in the context of fire simulations in future research.

3.3.3. Radiation modelling

When it comes to radiation modelling, different approaches exist, with a very wide range in complexity from the simplified radiative fraction approach, which neglects absorption, the use of a gray gas model, the weighted-sum-of-gray-gas (WSGGM) type of models and the more complete model which considers spectral dependency in the calculations.

Typically, in radiation modelling of fire scenarios, the radiative intensity is a function of both spatial location and angular direction, which then is obtained by solving the radiative transfer equation (RTE) using the finite volume discrete ordinates model (fvDOM). Within FireFOAM, a common approach for modelling absorption/emission is either the use of the constant radiative fraction approach [76, 77] (i.e., assuming an optically thin flame and neglecting absorption), or using the gray gas model with [78] and without [79] turbulence radiation interactions (TRI). Within FDS, the absorption coefficient of a gas mixture is typically calculated as a sum of individual gases' gray or band-mean absorption coefficients using a narrow-band model, RADCAL [80], with a correction, based on the radiative fraction approach, of the emission term in the flame region which is

necessary in the case of under-resolved fires. Nevertheless, the constant radiative fraction approach as well as the WSGGM and the wide band models are also available in the code [81]. The degree of complexity of radiation modelling in fire simulations can significantly vary depending on the scenario at hand and whether the simulations are aimed to be fully predictive or not. For example, the radiative fraction model has been used in the past for modelling flame extinction of a turbulent line burner [60]), as well as the WSGGM type of models [82] and line-by-line (LBL) spectral calculations [83] with a modified version of FDS.

Within the constant radiative fraction model, which considers a non-absorbing and optically thin medium, the radiative heat fluxes are calculated as:

$$\nabla \cdot \overline{\dot{q}_r} = \chi_r \overline{\dot{Q}_f'''} \quad (21)$$

where χ_r is a constant global radiative fraction for the fuel and the triple prime means 'per unit volume'. The advantage of this model is that it guarantees the desired amount of heat being released due to radiation and avoids the complexity of turbulence – radiation interaction, so that the evaluation of the combustion model can be done independently to any uncertainties related to simultaneously trying to predict the radiative fractions. In FDS, the radiative fraction approach does not rely on the optically thin assumption. Rather, it locally enforces the prescribed radiative fraction from the reaction zone, which is particularly useful when the flames are not resolved in detail (as is common in fire simulations): the effect of temperature errors due to such lack of resolution is mitigated.

The assumption of a (global) constant radiative fraction might not always be justified and can it can potentially lead to errors in the estimation of the heat fluxes on the fuel surface (i.e., heat feedback) in scenarios involving solid pyrolysis or liquid fuel evaporation. The WSGGM model is a compromise between the oversimplified gray gas model and a complete model which takes into account particular absorption bands, various forms of which exist in literature. Within a WSGGM type of model, the total emissivity and absorptivity (assuming $\alpha = \varepsilon$) of a gas mixture is calculated as the sum of fictitious gray gases weighted with a temperature dependent weighting factor as:

$$\varepsilon = \sum_{i=0}^I a_{\varepsilon,i}(T) (1 - e^{-\kappa_i p L}) \quad (22)$$

where $a_{\varepsilon,i}$ is the emissivity weight factor of the i fictitious gray gas, κ_i is the absorption coefficient of the i gray gas, p is the sum of the partial pressures of all absorbing gases and L is the path length, calculated as, e.g., $L = 3.6 V/A$ [37]. A usual approach is to assign a-priori a constant value for L or, alternatively, to allow it to vary during the simulations using a dynamic approach. In the latter, the volume, V , is calculated by summing all the cell volumes where reaction takes place. Assuming a certain flame shape (e.g., rectangular or conical

depending on the fuel source configuration), then the corresponding surface area, A , can be calculated.

The temperature dependence of $a_{\varepsilon,i}$ is given as:

$$a_{\varepsilon,i} = \sum_{i=0}^J b_{\varepsilon,i,j} \tilde{T}^{j-1} \quad (23)$$

where $b_{\varepsilon,i,j}$ are the emissivity gas temperature polynomial coefficients. The coefficients $b_{\varepsilon,i,j}$ and κ_i are taken from [84]. In the simplest approach, namely the 'gray' version of WSGG, the total absorptivity is then calculated as:

$$\alpha = -\frac{\ln(1 - \varepsilon)}{L} \quad (24)$$

and the radiative heat fluxes are calculated as:

$$\nabla \cdot \bar{q}_r'' = \alpha(4\sigma\tilde{T}^4 - \tilde{G}) \quad (25)$$

where σ is the Stefan-Boltzmann constant and G is the total irradiance.

It is important to note that fully decoupling turbulence modelling from combustion and radiation modelling in the context of reacting buoyant plume applications is not feasible. Care should be taken when reporting numerical predictions in order to make sure that all the different physical aspects have been correctly modelled (i.e., there are no non-physical solutions) and to try to minimize any compensating effects that could influence the numerical predictions. The use of non-dissipative numerical schemes is important to this respect. Additionally, reporting of the radiative fractions, when these are predicted in the numerical simulations, is also essential for a better evaluation of the predicted flame temperatures. Overall, comparing both local and global quantities is of great interest when it comes to fire modelling since the combination of both give a much better indication of the accuracy of the numerical modelling employed in a numerical study.

4. Low-frequency oscillatory behavior

4.1. The phenomenon

The focus here is on mechanically ventilated airtight compartments. As mentioned before, one important extensive experimental campaign was the PRISME project [4], and one, at the time unexpected, outcome was that for certain settings, low frequency oscillatory behavior was observed.

In the corner stone paper [85], this oscillatory phenomenon, with a period of up to 200 s (frequencies of 5 to 7 mHz), is explained through the coupled processes of burning rate, compartment pressure, ventilation flow rates, oxygen concentrations and heat feedback from the flames. It is worth noting that the fuel was liquid (dodecane and heptane) and until recently it was believed that the oscillatory behavior would not be observed for gaseous fuels. This point is discussed in section 4.3 of the paper, though.

An interesting finding in [85] is that the oscillatory behavior is only observed when the gas

temperature inside the compartment is sufficiently high and the oxygen concentration is sufficiently low (and not far from the extinction limit). The latter relates to the global equivalence ratio (GER), discussed below in section 4.2, and will have an impact on the HRR evolution through the ventilation conditions. It is also noted that the gas temperature links to the net heat gain/loss per unit time in the compartment, explained to be a key quantity in section 2.2.

Worth noting is that displacement of the flame, away from the fuel surface, is mentioned as an important feature for the oscillatory phenomena in [85]. Whereas for obvious reasons this has a very strong impact on the heat feedback, and hence, through evaporation, on the fuel mass loss rate and hence the HRR, it is interesting to observe that the CFD results in [85] predict oscillations (albeit with under-estimated amplitude and not with the correct frequency) in the absence of such flame displacement. This indicates that, whereas the flame displacement will surely have an impact on the amplitude, and possibly on the frequency, of the oscillations, it may not be necessary for oscillations to occur. This is addressed in section 4.3.

It is interesting to note that flame displacement (called 'ghosting flames'), oscillations and 'vent burning' have been described in [86], where a pan of liquid heptane fuel was ignited in a naturally ventilated compartment with limited ventilation openings. Oscillating flames were reported to 'represent the condition where the flame is shrinking to extinction, but cycles back to its original size' [86]. This observation illustrates that the oscillation phenomenon is not limited to mechanically ventilated compartments, and that with liquid fuels the heat feedback seems to be key. [As a side note, it is mentioned here that a frequency of 1Hz is reported in [86], but that might be limited by the scan rate, which had a period of 1 s.] Actually, the oscillatory phenomenon with natural ventilation was already reported more than 20 years earlier [87].

In [88] a distinction is made between unstable oscillating combustion, leading to extinction, and stable oscillating combustion, with methanol as fuel and with natural ventilation. Hydrodynamic instability is mentioned as cause of the oscillations, albeit not for the stable oscillating combustion. Nevertheless, this seems an interesting route to explore, given the current potential of CFD (see also section 4.3). It is also interesting to note that no link is found between the period of the oscillations (1 to 1.5 s in [88]) and the ventilation factor.

Interestingly, low-frequency oscillations were also observed with solid fuel in cable tray fire tests in the PRISME-2 campaign [89], where the assumption is developed that the combustion of accumulated unburnt gases causes the oscillations. This confirms the importance of the turbulent combustion process in the gas phase.

Coming back to the analysis of the PRISME tests as described in [85], a reduced-scale study was elaborated in the NYX set-up, with mechanical extraction and natural air supply [31]. Particularly appealing in [31] is the range of conditions tested:

the fuel type (variable volatility), pool size, air renewal rate and ventilation conditions (including variable position of the inlet of air). The study also reported extreme sensitivity: the mere presence of oxygen measurement devices was sufficient to significantly affect the oscillations and extinction phenomena. This is an important point of attention for experimental work in this field.

4.2. *Global equivalence ratio (GER)*

From section 2, it is obvious that the HRR evolution is very important with respect to the evolution of the fire-induced pressure. Hence a logical reasoning would be to try and find a link with the equivalence ratio, as this would have a strong impact on the completeness of combustion.

In [90], in the context of heptane pool fires in a box with natural ventilation through vents with variable width, different flame behavior regimes have been established and a GER value of around unity was reported to be indicative of oscillatory behavior. It is interesting to note, though, that the bottom horizontal vent, for the air supply, faced the fuel source, providing a relatively straight flow of air directly to the pool. This was not the case in, e.g., [31], and while the GER is still a relevant quantity, it is not sufficient to fully characterize the combustion regime inside. In fact, over the years more and more evidence has emerged that the GER is not sufficient to characterize the oscillatory behavior: knowledge of the flow field is essential to understand the combustion regime, as the flow field will determine the mixing of air and fuel vapor. This is discussed in more detail in section 4.3.

This said, the GER is still a very relevant parameter for combustion in mechanically ventilated confined compartments. It is useful to preserve this quantity when scaling configurations, as mentioned in [32].

4.3. *The importance of the flow field*

In [91], the importance of the flow field was illustrated very clearly for pool fires (with ethanol as fuel) in an ISO 9705 room with mechanical extraction and natural air supply. Modifying the position for the air supply duct from the upper to the lower position was shown to have a significant impact on the burning behavior. It was mentioned to be even one of the principal factors in [91]. This has been confirmed in [92], where it was even possible to change the fire regime from under-ventilated conditions to over-ventilated fires, only by modifying the position for the (natural) air intake from high to low. In the latter position, the air can mix with the combustible fuel vapor as released from the heptane pool much more easily and intensely than when the air intake is closer to the ceiling. With the high position, the stratification is also destroyed and the conditions become more like a well-stirred reactor [92]. This cannot be described by the GER, illustrating that knowledge of the GER alone is not sufficient to address the oscillatory behavior.

Also in [31] the importance of the flow field has been reported, in particular stating that ‘the

occurrence and persistency of low-frequency oscillations result from the competition between oxygen supply and fuel vapor supply due to the heat feedback from the flame and enclosure to the fuel tray.

Interestingly, the studies of [31] and [92] also contain CFD results. This is not surprising, given the increased computing power over the years. Worth mentioning in that respect is also the study of [93], where a detailed liquid evaporation model has been coupled to the gas phase solver, in the assumption that the evaporation model, through the supply of the combustible fuel vapor, plays a key role in the oscillation phenomenon. This point is addressed again in section 4.4 below. Yet, another very interesting finding in [93] is the importance of the position of the air inlet, related to the mixing and oxygen supply to the flame base. Indeed, it is concluded in [93] that both the evaporation model and the extinction model are key to predict oscillatory behavior with CFD. The latter is obviously a gas phase phenomenon, as discussed in section 3.2.

To conclude: given the importance of the flow field, combined with ever increasing computing power, it is expected that more detailed CFD studies will shed light on the oscillatory combustion behavior in the coming years. Recent examples are [94] (Fig. 12) or [92] (Fig. 20).

4.4. *Gas phase phenomenon?*

As mentioned above, the common assumption is that the oscillatory behavior is due to coupled evaporation and combustion. The flames, determined by the combustion in the gas phase, provide (together with the walls and the smoke layer or hot combustion products) the heat feedback to the liquid fuel surface, determining the evaporation rate. This creates a fuel mass loss rate into the gas phase, where the combustible gases mix with the oxygen to burn, creating the flames. This is then a closed loop.

This is clearly a plausible scenario: in [93], e.g., it was illustrated that both an evaporation model and an extinction model are required to predict oscillations, supporting the assumption. However, oscillations were found in the CFD results of [93] for configurations without oscillatory behavior in the experiments. This deserves further investigation.

A common assumption [85] in the described scenario is that the high-amplitude low-frequency oscillations are caused by flame displacement (‘ghosting flames’): when the flames move away from the fuel surface in locally under-ventilated conditions, looking for oxygen elsewhere in the compartment, the heat feedback to the fuel surface reduces significantly. This causes a strong reduction in fuel mass loss rate, hence HRR, leading to under-pressures (see section 2), increased oxygen supply from the ventilation system, creating well-ventilated conditions near the fuel surface and, if the temperature remains sufficiently high, the flame going back to the fuel surface, so a new cycle can start. Again, this is clearly a plausible scenario, observed in

experiments [31, 85]. Yet, the CFD results of [31] do not confirm this scenario, or at least indicate that ghosting flames are not required to obtain low-frequency oscillations with high amplitude: the correct frequency and amplitude of the fuel mass loss rate oscillations is found, but the model does not predict flame displacement.

In this light, the recent observation in [20, 21], shown here as Fig. 8, is very interesting, because this is a result from the extensive experimental campaign in the NYX set-up with propane as fuel (see section 2). In other words: there is no evaporation process here, while the oscillations are clearly observed. Admittedly, the amplitude (around 10 Pa) is an order of magnitude less than what is reported in Fig. 3 of [31], where heptane was used as fuel, in the same NYX set-up. That is not surprising, given the coupling to the evaporation process for the liquid fuel, but the observation that the evaporation process is not required for the oscillations to happen is remarkable and requires further investigation. Fig. 9 confirms the interaction of the pressure oscillations with oscillations in the admission and extraction flow rates, as was the case with liquid fuels.

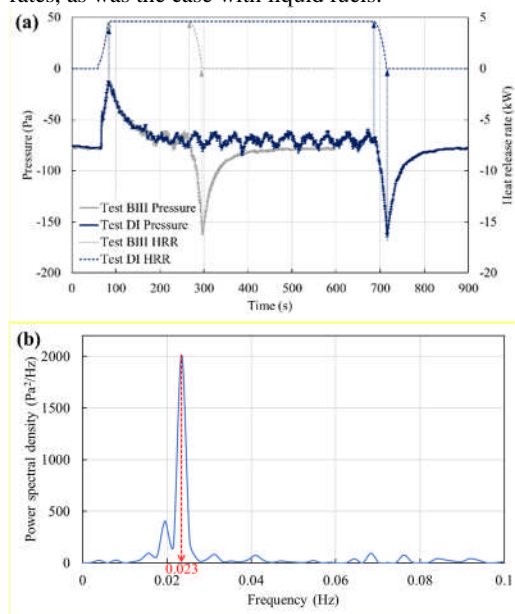


Fig. 8. (a) Low-frequency oscillatory behavior observed in Tests BIII and DI in [20]; (b) FFT analysis of the frequency during the steady-state of Test DI (dominant frequency of 23 mHz).

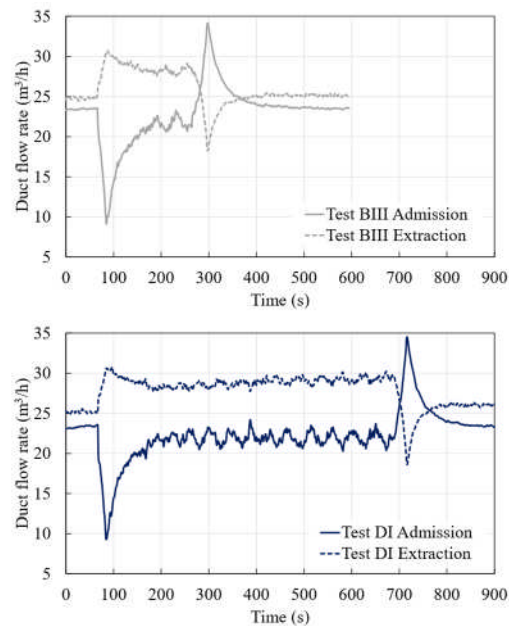


Fig. 9. Temporal evolutions of the ventilation flow rates in Tests BIII (top) and DI (bottom) [20].

It should be noted that no flame displacement was observed during the tests of [20, 21], so that is not the explanation. Indeed, the GER evolution (shown in Fig. 10) reveals well-ventilated conditions at all times. It is interesting to mention that the criterion of GER being around unity for oscillatory behaviour as mentioned in section 4.2 for naturally vented compartments, does not prevail here, either.

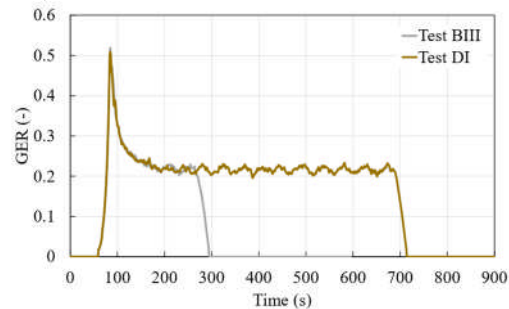


Fig. 10. GER evolutions of Tests BIII and DI [20].

Another striking observation concerns the (almost) identical frequency of the oscillations as reported in [31] for heptane as fuel (22.8 mHz), and as obtained from a FFT analysis in Fig. 8 (23 mHz) with propane as fuel, both in the same NYX set-up. The ventilation flow rates are very similar (28 m³/h in [31], versus 24 m³/h in [21]), as are the GER values, so the speculation that the transport/advection time of oxygen from the point of entry into the compartment to the fuel determines the frequency of the oscillations [31, 95], seems worth exploring.

As a final note, stressing the importance of further exploring the flow fields and gas phase phenomena in general, it is noted that the frequency as found in the NYX set-up (around 23 mHz) does not scale directly as expected from the full-scale set-up: in [85] a frequency of around 6mHz is reported in the DIVA set-up, with a geometrical scaling factor of 4. Based on $t \propto l^{1/2}$, the ratio of the frequencies would be expected to be 2, not 4. The fact that the frequency seems to scale with l could be a mere coincidence and requires more investigation (e.g., on the position and orientation of the air supply and gas extraction duct).

Based on these observations, it is suggested to explore the importance of the flow field in much more depth than has been done thus far. Fig. 11 and Fig. 12 show instantaneous velocity vectors in the vertical plane through the admission duct and the burner, respectively, at a few characteristic times for test DI. Whereas these plots are of qualitative value only, they do illustrate the complexity of the flow field, where the fire-induced buoyancy is certainly not the only driving force. E.g., in Fig. 11 it is seen that the over-pressure at $t = 100$ s leads to a reduced inflow of fresh air, whereas the opposite is observed at $t = 700$ s (under-pressure). The flow at $t = 800$ s provides an indication of the impact of the fire (i.e., the flow is shown in the absence of the fire, so the comparison can be made to the other contour plots). Fig. 12 shows the impact of the interaction of the mechanical ventilation with the fire-induced buoyancy: only relatively briefly a 'classical' fire plume is recognized (around $t = 100$ s, during the short fire growth stage), after which the upward velocity reduces and the plume is tilted, due to turbulent mixing.

To the very least, this shows that the flow field is very complex. More importantly, the fire-induced buoyancy is not the only driving force, and presumably is not the dominant force (see final note below). Given the maturity of CFD software, including the numerical schemes and models as they are, this opens up a very interesting research domain, namely the detailed study of the flow field and its effect on the fire dynamics inside compartments.

As a final note, it is mentioned that in the final configurations, with pressure and flow rate oscillations with the propane gas burner, there was no indication of fluctuations in the HRR: the mass flow rate was very stable (not shown) and the GER was always well below 1, indicating well-ventilated conditions at all times. Also, visually (see Fig. 1) there was no indication of reduced HRR at any point in time. This suggests that fluctuations in HRR (or mass loss rate) with liquid fuels, as mentioned above, might be the consequence of a flow phenomenon, rather than the cause or driver of the oscillations. This remains to be explored in the (near) future and again CFD, with detailed flow field analysis (e.g., through close examination of streamlines and transport times), could shed light on this.

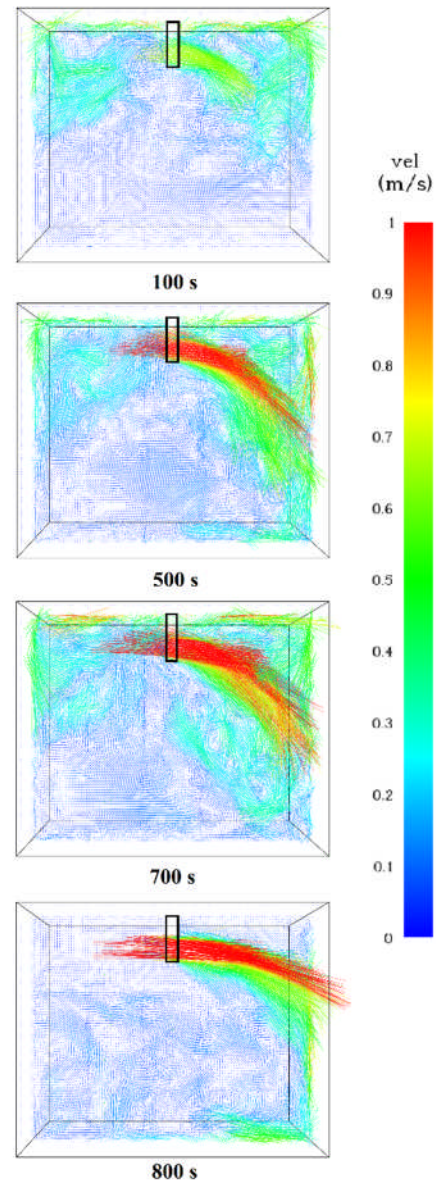


Fig. 11. Instantaneous velocity vectors in the vertical plane through the admission duct (indicated by black rectangles) at a few characteristic times for test DI ($t = 100$ s; 500 s; 700 s; 800 s).

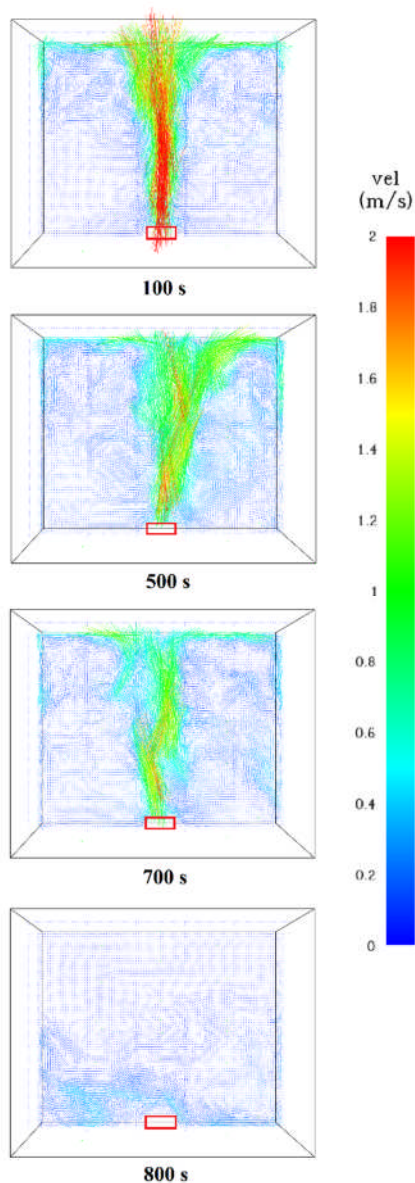


Fig. 12. Instantaneous velocity vectors in the vertical plane through the burner (indicated by red rectangles) at a few characteristic times for test DI ($t = 100$ s; 500 s; 700 s; 800 s).

5. Conclusions and perspectives

The background of the paper was an increased interest in fire dynamics in compartments with mechanical ventilation and limited leakage. Significant fire-induced pressure values, up to several hundreds of Pascal, are observed. This poses a practical problem, with relevance for fire safety science.

From the energy balance, the importance of the net heat gained per unit time in the gas phase was argued first. This led to the need to accurately quantify the heat release rate (HRR) inside the compartment as a function of time. Acknowledging practical complexities in experiments, the use of

gaseous fuel can be interesting, as this also allows for more flexibility in terms of variable HRR. However, the paper focuses on numerical simulations, in particular on CFD in the gas phase.

An overview was provided of turbulent combustion models as used today in the fire science community, with specific attention to the modelling of extinction and re-ignition. The latter is very important in the context of reliable CFD simulations, in particular when transient phenomena are in place. It has been argued that research on mixture fraction-based models with detailed chemistry might be worth exploring further. A 'proper' choice for the conditional scalar dissipation rate is key, acknowledging the important difference between buoyancy-driven, low SDR fire flames and momentum-driven, high SDR jet flames. This links to the importance of thermal quenching in fire simulations, where radiation is key. This involves soot as well, particularly if the radiative fractions are predicted in the modelling. Depending on the choices made for the turbulent combustion and radiation modeling, predictions of flame extinction can become strongly mesh sensitive, with a direct impact on the HRR. A few suggestions were made for the possibility dynamic modelling of turbulent combustion, coupled with radiation modelling.

A scaling analysis was presented as well. It has been highlighted that this is not trivial. Starting from the classical Froude similarity, the importance of correctly scaling of heat losses through boundaries has been confirmed. Even so, and even if the global equivalence ratio (GER) were conserved, it has been argued from the energy balance that the transient term in Eq. (6) does not scale in the same manner as the other terms. Consequently, while globally the fire induces pressure scales linearly with the geometry scale, care must be taken when analyzing fast variations in pressure. More detailed and systematic future research is needed to quantify the impact.

Finally, the interesting phenomenon of low-frequency oscillatory behavior of fire-induced pressures in airtight mechanically ventilated compartments has been discussed. It was brought about that, while the GER is a very relevant parameter, it is not sufficient to predict the combustion regime inside the compartment. Detailed knowledge on the flow field, determining the mixing of combustible fuel gases with oxygen near the fire source, is required. Therefore, it is expected that more detailed CFD studies will shed more light on the oscillatory combustion behavior in the coming years.

The oscillatory behavior can only be predicted if an accurate representation of the flow field is combined with accurate predictions of combustion (including extinction and reignition) and heat transfer (including radiation and soot). Until recently, the oscillations were believed to occur only with liquid fuel and the coupling with the evaporation process (and the modeling thereof) was deemed essential, but the phenomenon has now also been observed with a gaseous fuel (albeit with much smaller amplitude). Analysis of the

frequencies and GER values at reduced scale for different fuels, and at full scale (with the same fuel) confirms that more CFD studies are required, with finite rate combustion effects included.

From the complexity of the flow field, it was argued that the fire-induced buoyancy is not the only driving force, and presumably not the dominant force (see final note below). The maturity of existing CFD software opens up a very interesting research domain, namely the detailed study of the flow field and its effect on the fire dynamics inside compartments. This is not at all limited to configurations like the ones discussed in the present paper (i.e., air-tight mechanically ventilated compartments), but applies to any configuration where momentum plays a role. Examples are travelling fires, which arguably should be called ‘moving fires’ to indicate that the fire cannot ‘decide’ by itself where it travels as the air momentum, which depends on the ventilation settings, will also play a role (which may be dominant); large open plan fires; fires where the impact of wind is examined; and more. Detailed CFD simulations are expected to shed light on this in the foreseeable future.

6. Acknowledgements

The research of Dr. Junyi Li has been funded by China Scholarship Council (CSC, Grant No. 201706420076), as well as the co-funding from Ghent University through BOF (Grant No. 01SC2018). The research of Dr. Georgios Maragkos, reported in the paper, has been funded by Ghent University (Belgium) through GOA project BOF16/GOA/004. The authors would like to thank (in alphabetical order) Simo Hostikka, Randy McDermott, Hugues Pr  tre, Alexander Snegirev and Arnaud Trouv   for providing invaluable comments on the draft version of the paper.

7. References

[1] S. Hostikka, R.K. Janardhan, U. Riaz, T. Sikanen, Fire-induced pressure and smoke spreading in mechanically ventilated buildings with air-tight envelopes, *Fire Safety J*, 91 (2017) 380-388. <https://doi.org/10.1016/j.firesaf.2017.04.006>

[2] R.K. Janardhan, S. Hostikka, Experiments and Numerical Simulations of Pressure Effects in Apartment Fires, *Fire Technol*, 53 (2017) 1353-1377. <https://doi.org/10.1007/s10694-016-0641-z>

[3] H. Pr  tre, W. Le Saux, L. Audouin, Pressure variations induced by a pool fire in a well-confined and force-ventilated compartment, *Fire Safety J*, 52 (2012) 11-24. <https://doi.org/10.1016/j.firesaf.2012.04.005>

[4] L. Audouin, L. Rigollet, H. Pr  tre, W. Le Saux, M. Rowekamp, OECD PRISME project: Fires in confined and ventilated nuclear-type multi-compartments - Overview and main experimental results, *Fire Safety J*, 62 (2013) 80-101. <https://doi.org/10.1016/j.firesaf.2013.07.008>

[5] C. Fourneau, N. Cornil, C. Delvosalle, H. Breulet, S. Desmet, S. Brohez, Comparison of Fire

Hazards in Passive and Conventional Houses, *Cisap5: International Conference on Safety & Environment in Process & Power Industry*, Pt 1, 26 (2012) 375-380.

<https://doi.org/10.3303/Cet1226063>

[6] S. Brohez, P. Duhamel, Inwards doors blocked by fire induced overpressure in airtight apartment: a real case in Germany, *Chemical Engineering Transactions*, 67 (2018) 25-30.

<https://doi.org/10.3303/CET1867005>

[7] S. Brohez, I. Caravita, Overpressure induced by fires in airtight buildings, *Journal of Physics: Conference Series*, IOP Publishing, 2018.

<https://doi.org/10.1088/1742-6596/1107/4/042031>

[8] S. Brohez, I. Caravita, Fire Induced Pressure in Passive Houses: Experiments and FDS Validation, Ninth International Seminar on Fire and Explosion Hazards, Saint-Petersburg Polytechnic University Press, 2019. <https://doi.org/10.18720/spbpu/2/k19-132>

[9] S. Brohez, I. Caravita, Fire induced pressure in airtight houses: Experiments and FDS validation, *Fire Safety J*, 114 (2020) 103008.

<https://doi.org/10.1016/j.firesaf.2020.103008>

[10] R.G. Rehm, G.P. Forney, The Pressure Equations in Zone-Fire Modeling, *Fire Science and Technology*, 14 (1994) 61-73.

<https://doi.org/10.3210/fst.14.61>

[11] J.G. Quintiere, *Fundamentals of Fire Phenomena*, John Wiley & Sons Ltd, 2006.

[12] A.Y. Snegirev, L.T. Tanklevskii, The macrokinetics of indoor fire, *Teplofizika vysokikh temperatur (High Temperature)*, 36 (1998) 737-743.

<http://mi.mathnet.ru/eng/tvt2550>

[13] B. Karlsson, J. Quintiere, *Enclosure fire dynamics*, CRC press, 1999.

[14] J. Li, H. Pr  tre, S. Suard, T. Beji, B. Merci, Experimental study on the effect of mechanical ventilation conditions and fire dynamics on the pressure evolution in an air-tight compartment, *Fire Safety J*, 125 (2021) 103426.

<https://doi.org/10.1016/j.firesaf.2021.103426>

[15] J. Wahlqvist, P. van Hees, Evaluating methods for preventing smoke spread through ventilation systems using fire dynamics simulator, *Fire Mater*, 41 (2017) 625-645.

<https://doi.org/10.1002/fam.2404>

[16] J. Wahlqvist, P. van Hees, Validation of FDS for large-scale well-confined mechanically ventilated fire scenarios with emphasis on predicting ventilation system behavior, *Fire Safety J*, 62 (2013) 102-114. [10.1016/j.firesaf.2013.07.007](https://doi.org/10.1016/j.firesaf.2013.07.007)

[17] J. Li, T. Beji, S. Brohez, B. Merci, Experimental and numerical study of pool fire dynamics in an air-tight compartment focusing on pressure variation, *Fire Safety J*, 120 (2021) 103128.

<https://doi.org/10.1016/j.firesaf.2020.103128>

[18] J. Li, T. Beji, S. Brohez, B. Merci, CFD Study of Fire-Induced Pressure Variation in a Mechanically-Ventilated Air-Tight Compartment, *Fire Safety J*, 115 (2020).

<https://doi.org/10.1016/j.firesaf.2020.103012>

- [19] J. Li, H. Prêtre, S. Suard, T. Beji, B. Merci, Energy balance equation for pressure in air-tight compartment fires: detailed discussion and experimental validation, *Fire Safety J*, 122 (2021) 103362. <https://doi.org/10.1016/j.firesaf.2021.103362>
- [20] J. Li, H. Prêtre, T. Beji, B. Merci, Influence of fire heat release rate (HRR) evolutions on fire-induced pressure variations in air-tight compartments, *Fire Safety J*, (2021) 103450. <https://doi.org/10.1016/j.firesaf.2021.103450>
- [21] J. Li, Experimental and Numerical Study of Fire Dynamics in Air-Tight Buildings, PhD thesis, Ghent University, Ghent, Belgium, 2021.
- [22] NIST, Fire Dynamics Simulator (FDS) and Smokeview (SMV), (2021). <https://pages.nist.gov/fds-smv/>
- [23] H. Prêtre, W. Le Saux, L. Audouin, Determination of the heat release rate of large scale hydrocarbon pool fires in ventilated compartments, *Fire Safety J*, 62 (2013) 192-205. <https://dx.doi.org/10.1016/j.firesaf.2013.01.014>
- [24] J.G. Quintiere, Scaling applications in fire research, *Fire Safety J*, 15 (1989) 3-29. [https://doi.org/10.1016/0379-7112\(89\)90045-3](https://doi.org/10.1016/0379-7112(89)90045-3)
- [25] J.G. Quintiere, Scaling realistic fire scenarios, *Progress in Scale Modeling, an International Journal*, 1 (2020) 1. <https://doi.org/10.13023/psmij.2020.01>
- [26] M.M. Barsim, M.A. Bassily, H.M. El-Batsh, Y.A. Rihan, M.M. Sherif, Froude scaling modeling in an Atrium Fire equipped with natural and transient forced ventilation, *Int J Vent*, 19 (2020) 201-223. <https://doi.org/10.1080/14733315.2019.1615220>
- [27] M. Wang, J. Perricone, P.C. Chang, J.G. Quintiere, Scale modeling of compartment fires for structural fire testing, *Journal of Fire Protection Engineering*, 18 (2008) 223-240. <https://doi.org/10.1177/1042391508093337>
- [28] W. Węgrzyński, P. Antosiewicz, T. Burdzy, M. Zimny, A. Krasuski, Smoke Obscuration Measurements in Reduced-Scale Fire Modelling Based on Froude Number Similarity, *Sensors*, 19 (2019) 3628. <https://doi.org/10.3390/s19163628>
- [29] F.A. Williams, 'Scaling Mass Fires' in *Fire Research Abstracts and Reviews*, Volume 11, The National Academies Press, Washington, DC, 1969. <https://doi.org/10.17226/18860>
- [30] M.J. Hurley, D.T. Gottuk, J.R. Hall Jr, K. Harada, E.D. Kuligowski, M. Puchovsky, J. Torero, J.M. Watts Jr, C.J. WIECZOREK, SFPE handbook of fire protection engineering, Fifth ed., Springer, 2016.
- [31] M. Mense, Y. Pizzo, H. Prêtre, C. Lallemand, B. Porterie, Experimental and numerical study on low-frequency oscillating behaviour of liquid pool fires in a small-scale mechanically-ventilated compartment, *Fire Safety J*, 108 (2019) 102824. <https://doi.org/10.1016/j.firesaf.2019.102824>
- [32] H. Prêtre, L. Bouaza, S. Suard, Multi-scale analysis of the under-ventilated combustion regime for the case of a fire event in a confined and mechanically ventilated compartment, *Fire Safety J*, 120 (2021) 103069. <https://doi.org/10.1016/j.firesaf.2020.103069>
- [33] K. McGrattan., S. Hostikka., J. Floyd., R. McDermott., M. Vanella., *Fire Dynamics Simulator User's Guide* (version 6.7.5), Sixth ed., NIST and VTT., 2020. <http://dx.doi.org/10.6028/NIST.SP.1019>
- [34] MaCFP, <https://github.com/MaCFP/macfp-db>, Access on: 2021.
- [35] A. Brown, M. Bruns, M. Gollner, J. Hewson, G. Maragkos, A. Marshall, R. McDermott, B. Merci, T. Rogaume, S. Stolarov, Proceedings of the first workshop organized by the IAFSS Working Group on Measurement and Computation of Fire Phenomena (MaCFP), *Fire Safety J*, 101 (2018) 1-17. <https://doi.org/10.1016/j.firesaf.2018.08.009>
- [36] FMGlobal, <https://github.com/fireFoam-dev>, Access on: 2021.
- [37] G. Maragkos, T. Beji, B. Merci, Towards predictive simulations of gaseous pool fires, *P Combust Inst*, 37 (2019) 3927-3934. <https://doi.org/10.1016/j.proci.2018.05.162>
- [38] G. Maragkos, B. Merci, On the use of dynamic turbulence modelling in fire applications, *Combust Flame*, 216 (2020) 9-23. <https://doi.org/10.1016/j.combustflame.2020.02.012>
- [39] B.F. Magnussen, B.H. Hjertager, On mathematical modeling of turbulent combustion with special emphasis on soot formation and combustion, 16 (1977) 719-729. [https://doi.org/10.1016/S0082-0784\(77\)80366-4](https://doi.org/10.1016/S0082-0784(77)80366-4)
- [40] J.X. Wen, L.Y. Huang, J. Roberts, The effect of microscopic and global radiative heat exchange on the field predictions of compartment fires, *Fire Safety J*, 36 (2001) 205-223. [https://doi.org/10.1016/S0379-7112\(00\)00058-8](https://doi.org/10.1016/S0379-7112(00)00058-8)
- [41] A.C.Y. Yuen, G.H. Yeoh, V. Timchenko, S.C.P. Cheung, T.J. Barber, Importance of detailed chemical kinetics on combustion and soot modelling of ventilated and under-ventilated fires in compartment, *Int J Heat Mass Tran*, 96 (2016) 171-188. <https://doi.org/10.1016/j.ijheatmasstransfer.2016.01.026>
- [42] A.C.Y. Yuen, G.H. Yeoh, V. Timchenko, T.B.Y. Chen, Q.N. Chan, C. Wang, D.D. Li, Comparison of detailed soot formation models for sooty and non-sooty flames in an under-ventilated ISO room, *Int J Heat Mass Tran*, 115 (2017) 717-729. <https://doi.org/10.1016/j.ijheatmasstransfer.2017.08.074>
- [43] A. Marchand, S. Verma, R. Xu, J. White, A. Marshall, T. Rogaume, F. Richard, J. Luche, A. Trouvé, Simulations of a turbulent line fire with a steady flamelet combustion model coupled with models for non-local and local gas radiation effects, *Fire Safety J*, 106 (2019) 105-113. <https://doi.org/10.1016/j.firesaf.2019.04.011>
- [44] R. Xu, A. Marchand, S. Verma, T. Rogaume, F. Richard, J. Luche, A. Trouvé, Simulations of the

- coupling between combustion and radiation in a turbulent line fire using an unsteady flamelet model, *Fire Safety J*, 120 (2021) 103101. <https://doi.org/10.1016/j.firesaf.2020.103101>
- [45] B. Kruljevic, I. Stankovic, B. Merci, Large eddy simulations of the UMD line burner with the conditional moment closure method, *Fire Safety J*, 116 (2020) 103206. <https://doi.org/10.1016/j.firesaf.2020.103206>
- [46] L. Ma, F. Nmira, J.-L. Consalvi, Large Eddy Simulation of medium-scale methanol pool fires-effects of pool boundary conditions, *Combust Flame*, 222 (2020) 336-354. <https://doi.org/10.1016/j.combustflame.2020.09.007>
- [47] F. Nmira, L. Ma, J.-L. Consalvi, Assessment of subfilter-scale turbulence-radiation interaction in non-luminous pool fires, *P Combust Inst*, 38 (2021) 4927-4934. <https://doi.org/10.1016/j.proci.2020.06.271>
- [48] N. Peters, Laminar diffusion flamelet models in non-premixed turbulent combustion, *Progress in energy and combustion science*, 10 (1984) 319-339. [https://doi.org/10.1016/0360-1285\(84\)90114-X](https://doi.org/10.1016/0360-1285(84)90114-X)
- [49] N. Peters, *Turbulent Combustion*, Cambridge University Press, 2000.
- [50] R. Xu, V. Minh Le, A. Marchand, T. Rogaume, F. Richard, J. Luche, A. Trouvé, The unsteady response of radiating laminar diffusion flames exposed to decreasing mixing rate conditions representative of fires, *Combustion Theory and Modelling*, 25 (2021) 1-21. <https://doi.org/10.1080/13647830.2020.1823021>
- [51] H. Pitsch, M. Chen, N. Peters, Unsteady flamelet modeling of turbulent hydrogen-air diffusion flames, *Symposium (International) on Combustion*, 27 (1998) 1057-1064. [https://doi.org/10.1016/S0082-0784\(98\)80506-7](https://doi.org/10.1016/S0082-0784(98)80506-7)
- [52] A. Giusti, M. Kotzagianni, E. Mastorakos, LES/CMC simulations of swirl-stabilised ethanol spray flames approaching blow-off, *Flow, turbulence and combustion*, 97 (2016) 1165-1184. <https://doi.org/10.1007/s10494-016-9762-1>
- [53] A.Y. Klimenko, R.W. Bilger, Conditional moment closure for turbulent combustion, *Progress in energy and combustion science*, 25 (1999) 595-687. [https://doi.org/10.1016/S0360-1285\(99\)00006-4](https://doi.org/10.1016/S0360-1285(99)00006-4)
- [54] B. Kruljevic, I. Stankovic, B. Merci, Systematic study of the impact of chemistry and radiation on extinction and carbon monoxide formation at low scalar dissipation rates, *Fire Safety J*, 117 (2020) 103212. <https://doi.org/10.1016/j.firesaf.2020.103212>
- [55] B. Cuenot, F.N. Egolfopoulos, T. Poinso, An unsteady laminar flamelet model for non-premixed combustion, *Combustion Theory and Modelling*, 4 (2000) 77-97. <https://doi.org/10.1088/1364-7830/4/1/305>
- [56] V. Lecoustre, P. Narayanan, H.R. Baum, A. Trouve, Local extinction of diffusion flames in fires, *Fire Safety Science*, 10 (2011) 583-595. <http://dx.doi.org/10.3801/IAFSS.FSS.10-583>
- [57] A. Linan, The asymptotic structure of counterflow diffusion flames for large activation energies, *Acta Astronautica*, 1 (1974) 1007-1039. [https://doi.org/10.1016/0094-5765\(74\)90066-6](https://doi.org/10.1016/0094-5765(74)90066-6)
- [58] S. Vilfayeau, J.P. White, P.B. Sunderland, A.W. Marshall, A. Trouvé, Large eddy simulation of flame extinction in a turbulent line fire exposed to air-nitrogen co-flow, *Fire Safety J*, 86 (2016) 16-31. <https://doi.org/10.1016/j.firesaf.2016.09.003>
- [59] Z. Hu, Y. Utiskul, J.G. Quintiere, A. Trouve, Towards large eddy simulations of flame extinction and carbon monoxide emission in compartment fires, *P Combust Inst*, 31 (2007) 2537-2545. <https://doi.org/10.1016/j.proci.2006.08.053>
- [60] J.P. White, S. Vilfayeau, A.W. Marshall, A. Trouve, R.J. McDermott, Modeling flame extinction and reignition in large eddy simulations with fast chemistry, *Fire Safety J*, 90 (2017) 72-85. <https://doi.org/10.1016/j.firesaf.2017.04.023>
- [61] J.C. Hewson, S.R. Tieszen, W.D. Sundberg, P.E. Desjardin, CFD modeling of fire suppression and its role in optimizing suppressant distribution, (2003). https://tsapps.nist.gov/publication/get_pdf.cfm?pub_id=909424
- [62] A.Y. Snegirev, A.S. Tsoy, Treatment of local extinction in CFD fire modeling, *P Combust Inst*, 35 (2015) 2519-2526. <https://doi.org/10.1016/j.proci.2014.07.051>
- [63] A.Y. Snegirev, Perfectly stirred reactor model to evaluate extinction of diffusion flame, *Combust Flame*, 162 (2015) 3622-3631. <https://doi.org/10.1016/j.combustflame.2015.06.012>
- [64] S.B. Dorofeev, Thermal quenching of mixed eddies in non-premixed flames, *P Combust Inst*, 36 (2017) 2947-2954. <https://doi.org/10.1016/j.proci.2016.06.061>
- [65] S.B. Pope, PDF methods for turbulent reactive flows, *Progress in energy and combustion science*, 11 (1985) 119-192. [https://doi.org/10.1016/0360-1285\(85\)90002-4](https://doi.org/10.1016/0360-1285(85)90002-4)
- [66] G. Maragkos, B. Merci, Large eddy simulations of flame extinction in a turbulent line burner, *Fire Safety J*, 105 (2019) 216-226. <https://doi.org/10.1016/j.firesaf.2019.03.008>
- [67] S.B. Pope, *Turbulent flows*, Cambridge University Press, 2000. <https://doi.org/10.1017/CBO9780511840531>
- [68] M. Faghri, B. Sundén, *Transport phenomena in fires*, WIT press, 2008.
- [69] P. Moin, K. Squires, W. Cabot, S. Lee, A dynamic subgrid-scale model for compressible turbulence and scalar transport, *Physics of Fluids A: Fluid Dynamics*, 3 (1991) 2746-2757. <https://doi.org/10.1063/1.858164>
- [70] J.W. Deardorff, Stratocumulus-capped mixed layers derived from a three-dimensional model, *Boundary-Layer Meteorology*, 18 (1980) 495-527. <https://doi.org/10.1007/BF00119502>
- [71] J. Bardina, J. Ferziger, W. Reynolds, Improved subgrid-scale models for large-eddy simulation,

- 13th fluid and plasmadynamics conference, (1980) 1357. <https://doi.org/10.2514/6.1980-1357>
- [72] F. Nicoud, F. Ducros, Subgrid-scale stress modelling based on the square of the velocity gradient tensor, *Flow, turbulence and Combustion*, 62 (1999) 183-200. <https://doi.org/10.1023/A:1009995426001>
- [73] A. Parente, M.R. Malik, F. Contino, A. Cuoci, B.B. Dally, Extension of the Eddy Dissipation Concept for turbulence/chemistry interactions to MILD combustion, *Fuel*, 163 (2016) 98-111. <https://doi.org/10.1016/j.fuel.2015.09.020>
- [74] R.J. McDermott, K.B. McGrattan, J.E. Floyd, A simple reaction time scale for under-resolved fire dynamics, Tenth International Symposium on Fire Safety Science, (2011) 809-820.
- [75] S. Menon, A.R. Kerstein, The linear-eddy model, in: *Turbulent combustion modeling*, Springer, 2011, pp. 221-247. https://doi.org/10.1007/978-94-007-0412-1_10
- [76] Y. Wang, P. Chatterjee, J.L. de Ris, Large eddy simulation of fire plumes, *P Combust Inst*, 33 (2011) 2473-2480. <https://doi.org/10.1016/j.proci.2010.07.031>
- [77] S. Vilfayeau, N. Ren, Y. Wang, A. Trouvé, Numerical simulation of under-ventilated liquid-fueled compartment fires with flame extinction and thermally-driven fuel evaporation, *P Combust Inst*, 35 (2015) 2563-2571. <https://doi.org/10.1016/j.proci.2014.05.072>
- [78] P. Chatterjee, Y. Wang, K.V. Meredith, S.B. Dorofeev, Application of a subgrid soot-radiation model in the numerical simulation of a heptane pool fire, *P Combust Inst*, 35 (2015) 2573-2580. <https://doi.org/10.1016/j.proci.2014.05.045>
- [79] S. Vilfayeau, Large eddy simulation of fire extinction phenomena, University of Maryland, College Park, 2015. <https://doi.org/10.13016/M2QB0M>
- [80] W.L. Grosshandler, RADCAL: A narrow-band model for radiation calculations in a combustion, Environment NIST Tech. Note, (1993). <https://nvlpubs.nist.gov/nistpubs/Legacy/TN/nbstechnicalnote1402.pdf>
- [81] K. McGrattan., S. Hostikka., J. Floyd., R. McDermott., M. Vanella., *Fire Dynamics Simulator Technical Reference Guide Volume 1: Mathematical Model*, NIST Special Publication 1018-1, 2021. <http://dx.doi.org/10.6028/NIST.SP.1018>
- [82] H. Sadeghi, S. Hostikka, G.C. Fraga, H. Bordbar, Weighted-sum-of-gray-gases models for non-gray thermal radiation of hydrocarbon fuel vapors, CH₄, CO and soot, *Fire Safety J*, 125 (2021) 103420. <https://doi.org/10.1016/j.firesaf.2021.103420>
- [83] H. Bordbar, S. Hostikka, P. Boulet, G. Parent, Numerically resolved line by line radiation spectrum of large kerosene pool fires, *Journal of Quantitative Spectroscopy and Radiative Transfer*, 254 (2020) 107229. <https://doi.org/10.1016/j.jqsrt.2020.107229>
- [84] L.J. Dorigon, G. Duciak, R. Brittes, F. Cassol, M. Galarca, F.H.R. Franca, WSGG correlations based on HITEMP2010 for computation of thermal radiation in non-isothermal, non-homogeneous H₂O/CO₂ mixtures, *Int J Heat Mass Tran*, 64 (2013) 863-873. <https://doi.org/10.1016/j.ijheatmasstransfer.2013.05.010>
- [85] H. Pretrel, S. Suard, L. Audouin, Experimental and numerical study of low frequency oscillatory behaviour of a large-scale hydrocarbon pool fire in a mechanically ventilated compartment, *Fire Safety J*, 83 (2016) 38-53. <https://doi.org/10.1016/j.firesaf.2016.04.001>
- [86] Y. Utiskul, J.G. Quintiere, A.S. Rangwala, B.A. Ringwelski, K. Wakatsuki, T. Naruse, Compartment fire phenomena under limited ventilation, *Fire Safety J*, 40 (2005) 367-390. <https://doi.org/10.1016/j.firesaf.2005.02.002>
- [87] H. Takeda, Oscillatory phenomenon and inverse temperature profile appearing in compartment fires, *Combust Flame*, 61 (1985) 103-105. [https://doi.org/10.1016/0010-2180\(85\)90076-8](https://doi.org/10.1016/0010-2180(85)90076-8)
- [88] K.I. Kim, H. Ohtani, Y. Uehara, Experimental study on oscillating behaviour in a small-scale compartment fire, *Fire Safety J*, 20 (1993) 377-384. [https://doi.org/10.1016/0379-7112\(93\)90056-V](https://doi.org/10.1016/0379-7112(93)90056-V)
- [89] P. Zavaleta, L. Audouin, Cable tray fire tests in a confined and mechanically ventilated facility, *Fire Mater*, 42 (2018) 28-43. <https://doi.org/10.1002/fam.2454>
- [90] Z. Hu, Y. Utiskul, J.G. Quintiere, A. Trouve, A comparison between observed and simulated flame structures in poorly ventilated compartment fires, *Fire Safety Science-Proceedings of the Eighth International Symposium*, (2005) 1193-1204.
- [91] K. Matsuyama, S. Okinaga, Y. Hattori, H. Suto, Experimental study on fire behavior in a compartment under mechanical ventilated conditions: the effects of air inlet position, in: *Fire Science and Technology 2015*, Springer, 2017, pp. 111-119. https://doi.org/10.1007/978-981-10-0376-9_11
- [92] L. Acherar, H.-Y. Wang, J.-P. Garo, B. Coudour, Impact of air intake position on fire dynamics in mechanically ventilated compartment, *Fire Safety J*, 118 (2020) 103210. <https://doi.org/10.1016/j.firesaf.2020.103210>
- [93] T. Sikanen, S. Hostikka, Predicting the heat release rates of liquid pool fires in mechanically ventilated compartments, *Fire Safety J*, 91 (2017) 266-275. <https://dx.doi.org/10.1016/j.firesaf.2017.03.060>
- [94] J.F.P. Segovia, T. Beji, B. Merci, CFD simulations of pool fires in a confined and ventilated enclosure using the Peatross-Beyler correlation to calculate the mass loss rate, *Fire Technol*, 53 (2017) 1669-1703. <https://doi.org/10.1007/s10694-017-0654-2>
- [95] J.F.P. Segovia, Numerical study on oscillatory fire behaviour in confined and mechanically-ventilated enclosures, PhD Thesis, Ghent

University, Ghent, Belgium, 2019.
<https://biblio.ugent.be/publication/8673553>